



OPEN

Adaptive immunity and neutralizing antibodies against SARS-CoV-2 variants of concern following vaccination in patients with cancer: the CAPTURE study

Annika Fendler ^{1,39}, Scott T. C. Shepherd ^{1,2,39}, Lewis Au ^{1,2,39}, Katalin A. Wilkinson ^{3,4,39}, Mary Wu ^{5,39}, Fiona Byrne¹, Maddalena Cerrone ^{3,6}, Andreas M. Schmitt², Nalinie Joharatnam-Hogan², Benjamin Shum^{1,2}, Zayd Tippu², Karolina Rzeniewicz¹, Laura Amanda Boos ², Ruth Harvey⁷, Eleanor Carlyle², Kim Edmonds², Lyra Del Rosario², Sarah Sarker², Karla Lingard², Mary Mangwende², Lucy Holt², Hamid Ahmod², Justine Korteweg², Tara Foley², Jessica Bazin⁸, William Gordon ¹, Taja Barber¹, Andrea Emslie-Henry¹, Wenyi Xie¹, Camille L. Gerard¹, Daqi Deng¹, Emma C. Wall ^{9,10}, Ana Agua-Doce¹¹, Sina Namjou¹², Simon Caidan¹², Mike Gavrielides¹³, James I. MacRae ¹⁴, Gavin Kelly ¹⁵, Kema Peat², Denise Kelly², Aida Murra², Kayleigh Kelly², Molly O'Flaherty², Lauren Dowdie², Natalie Ash², Firza Gronthoud¹⁶, Robyn L. Shea ^{16,17}, Gail Gardner¹⁶, Darren Murray¹⁶, Fiona Kinnaird¹⁸, Wanyuan Cui ¹⁹, Javier Pascual ²⁰, Simon Rodney², Justin Mencil ²¹, Olivia Curtis ¹⁹, Clemency Stephenson⁸, Anna Robinson⁸, Bhavna Oza², Sheima Farag², Isla Leslie², Aljosja Rogiers², Sunil Iyengar⁸, Mark Ethell⁸, Christina Messiou²², David Cunningham ²¹, Ian Chau ²¹, Naureen Starling²¹, Nicholas Turner²⁰, Liam Welsh²³, Nicholas van As²⁴, Robin L. Jones²⁵, Joanne Droney²⁶, Susana Banerjee²⁷, Kate C. Tatham²⁸, Mary O'Brien¹⁹, Kevin Harrington^{29,30}, Shreerang Bhide^{29,30}, Alicia Okines^{20,31}, Alison Reid³², Kate Young², Andrew J. S. Furness², Lisa Pickering ², Charles Swanton ^{33,34}, The Crick COVID-19 Consortium*, Sonia Gandhi^{35,36}, Steve Gamblin ¹⁰, David L. V. Bauer ³⁷, George Kassiotis ³⁸, Sacheen Kumar ²¹, Nadia Yousaf ^{19,31}, Shaman Jhanji ²⁸, Emma Nicholson⁸, Michael Howell⁵, Susanna Walker²⁸, Robert J. Wilkinson^{3,4,6}, James Larkin², Samra Turajlic ^{1,2} and The CAPTURE Consortium*

Coronavirus disease 2019 (COVID-19) antiviral response in a pan-tumor immune monitoring (CAPTURE) (NCT03226886) is a prospective cohort study of COVID-19 immunity in patients with cancer. Here we evaluated 585 patients following administration of two doses of BNT162b2 or AZD1222 vaccines, administered 12 weeks apart. Seroconversion rates after two doses were 85% and 59% in patients with solid and hematological malignancies, respectively. A lower proportion of patients had detectable titers of neutralizing antibodies (NAbT) against severe acute respiratory syndrome coronavirus 2 (SARS-CoV-2) variants of concern (VOC) versus wild-type (WT) SARS-CoV-2. Patients with hematological malignancies were more likely to have undetectable NAbT and had lower median NAbT than those with solid cancers against both SARS-CoV-2 WT and VOC. By comparison with individuals without cancer, patients with hematological, but not solid, malignancies had reduced neutralizing antibody (NAb) responses. Seroconversion showed poor concordance with NAbT against VOC. Previous SARS-CoV-2 infection boosted the NAb response including against VOC, and anti-CD20 treatment was associated with undetectable NAbT. Vaccine-induced T cell responses were detected in 80% of patients and were comparable between vaccines or cancer types. Our results have implications for the management of patients with cancer during the ongoing COVID-19 pandemic.

The ongoing evolution of SARS-CoV-2 has led to the emergence of VOC that have potentially enhanced transmission, pathogenicity and immune escape¹. Additionally, mutations

affecting spike (S) epitopes could reduce protection induced by vaccines developed based on the WT S protein. The highly infectious Delta VOC (B.1.167.2), first identified in India in early 2021,

A full list of affiliations appears at the end of the paper.

is currently the predominant variant worldwide. Despite its surging prevalence, it is suggested that vaccination programs have broken the link between infection and hospitalization and death², with many countries lifting COVID-19 restrictions. In the UK, however, those classified as clinically extremely vulnerable are still advised to take additional precautions of their own accord³, without clear communication regarding immune response to vaccines or vaccine efficacy around individual conditions within this heterogeneous clinical group. Furthermore, vulnerable patients were shown to be disproportionately affected by vaccine breakthrough infections⁴. In one study of 152 double-vaccinated patients hospitalized due to COVID-19, 40% were immunosuppressed (19% from chronic corticosteroid treatment, 18% from chemotherapy or antimetabolite treatment, 11% from solid organ transplant, 7% from anti-CD20 treatment), and overall cohort mortality was 22%⁵. Recently, preliminary results on BNT162b2 and AZD1222 vaccine effectiveness in extremely clinically vulnerable patients in England showed strong S-reactive antibody responses and vaccine effectiveness against symptomatic COVID-19 in all vulnerable groups except the immunocompromised, particularly after a single dose⁶.

Patients with cancer represent an important vulnerable group (an estimated 19.3 million new cancer diagnoses are made per year globally⁷) with an increased likelihood of poor clinical outcomes from COVID-19 (refs. ^{8–11}). As such, patients with cancer have been prioritized in COVID-19 vaccination programs globally^{12,13}; however, as they were virtually excluded from pivotal vaccine studies, data on efficacy or immune response to COVID-19 vaccines in this population are lacking. Given that cancer or its treatment may impact immunity, characterization of the immune response to COVID-19 vaccines in patients with cancer is a priority. Available studies demonstrated generally high seroconversion rates after two vaccine doses in patients with solid cancers ($\geq 90\%$, measured as immunoglobulin (Ig) G levels)^{14–17}, with less pronounced responses in those with hematological malignancies (compounded by treatments including anti-CD20 therapy)^{14,18–23}. However, data on functionally relevant SARS-CoV-2 NAb responses, particularly to VOC, are scarce. Vaccine-induced T cell responses have been reported in patients with cancer^{15,24}, but, again, activity against VOC is unknown. Furthermore, although humoral and cellular responses to SARS-CoV-2 often correlate²⁵, this has not been assessed regarding COVID-19 vaccines nor investigated in patients with cancer specifically. Finally, the effect of previous infection on subsequent vaccine-induced immunity in patients with cancer remains unclear. In the context of emerging VOC, such data are urgently needed to calibrate risk-mitigation measures and tailor vaccine regimes for patients with cancer.

The CAPTURE study is a prospective, longitudinal cohort study evaluating the impact of cancer and anticancer treatment on the immune response to SARS-CoV-2 infection and COVID-19 vaccinations²⁶. Data from the infection cohort (companion paper²⁷) show that the majority of patients with solid cancer develop durable humoral responses (of at least 11 months) and have detectable T cell responses to SARS-CoV-2 infection, but patients with hematological malignancies often display a discordance between humoral and cellular arms (owing to disease-related lineage defects and anti-CD20 treatment); additionally, neutralizing activity against Alpha, Beta and Delta VOC is reduced following infection with the WT SARS-CoV-2 strain. Here, we investigate whether humoral and cellular immunity is efficiently induced following COVID-19 vaccination in the vaccine cohort of the CAPTURE study, especially regarding VOC. Of note, this study was conducted in the UK, where the vaccination schedule initially followed an off-label 12-week interval between doses. This approach was implemented by the UK government during the second wave of the pandemic to maximize the number of people vaccinated with at least one dose.

Results

Cohort characteristics and COVID-19 vaccination. Between May 2020 and June 2021 (database lock), we recruited 626 patients with cancer who received at least one COVID-19 vaccine dose, of whom 41 (7%) had no follow-up samples and were excluded from the analysis (Extended Data Fig. 1a and Table 1). Of the 585 evaluable patients, 93% received two vaccine doses; 74% (430 of 585) received the AZD1222 vaccine (Oxford–AstraZeneca (AZ)) and 26% (153 of 585) received the BNT162b2 vaccine (Pfizer–BioNTech (PZ)). Overall, 93% (546 of 585) received the second dose at a median of 77 d (interquartile range (IQR), 72–78 d) in accordance with guidance for the 12-week interval between vaccine doses¹³. Five percent of patients (29 of 585) did not receive a second vaccine dose due to either cancer-related death (3%, 16 of 585), clinical advice (1%, 7 of 585) or patient preference (1%, 6 of 585), and 2% of patients (10 of 585) either withdrew study consent or were lost to follow-up (Table 1 and Extended Data Fig. 1a). There were no baseline differences between patients who were included or excluded from the final analysis nor between patients receiving one or two vaccine doses (Supplementary Table 1). Restrictions on hospital attendance during the pandemic resulted in a small number of missed follow-up samples (Extended Data Fig. 1b and Supplementary Table 2).

The median age of patients was 60 years (IQR, 52–68 years), and 60% (323 of 585) of patients were male. Overall, 69% of patients (404 of 585) were naive to SARS-CoV-2 infection and 31% of patients (181 of 585) had prior SARS-CoV-2 infection confirmed either by PCR with reverse transcription (RT-PCR) for SARS-CoV-2 (median time from positive test to baseline of 77 d (IQR, 40–287 d)) or the presence of S1-reactive antibodies at baseline. In total, 76% of patients (447 of 585) had a current diagnosis of solid cancer and 24% of patients (138 of 585) had hematological malignancies. The majority of patients with solid cancers had metastatic disease (68% (306 of 447)) (Table 1). Patients receiving PZ were more likely to be older (median of 63 years versus 59 years with AZ, $P < 0.001$) and to have a hematological malignancy (35% with PZ versus 23% with AZ, $P = 0.02$), reflecting earlier licensing of PZ and prioritization of these groups as extremely clinically vulnerable. Patients with hematological malignancies were more likely to be male (60% versus 55% with solid cancers, $P = 0.01$), and patients receiving PZ were more likely to have had prior SARS-CoV-2 infection (Supplementary Table 3).

Overall, 21% of patients (123 of 585) received treatment with chemotherapy, 34% of patients (200 of 585) received treatment with targeted therapy, and 3% of patients (20 of 585) received treatment with endocrine therapy within 28 d before vaccination. Thirty-one percent of patients (185 of 585) received immune-checkpoint inhibitors (CPI), with 19% of patients (109 of 585) receiving CPI treatment within 183 d of vaccination; 22% of patients (24 of 109) had active immune-related adverse events secondary to CPI, although only 4% of patients (4 of 109) received immunosuppression with corticosteroids (equivalent of > 10 mg prednisolone for ≥ 7 d) within 48 h of vaccination.

In total, 4% of patients (26 of 585) received anti-CD20 therapy within 12 months of vaccination and 10% of patients (58 of 585) previously received hematological stem cell transplant (43%, allogeneic (25 of 58); 57%, autologous (33 of 58)), of which 16% (9 of 58) were within 6 months of vaccination; 31% of patients (18 of 58) had active graft-versus-host disease requiring immunosuppression at the time of vaccination. Five percent (32 of 585) of patients had radiotherapy or surgery within 28 d of vaccination.

At the time of vaccination, 7% of patients (39 of 585) were receiving immunosuppressive therapy with corticosteroids (5% (29 of 585); equivalent of > 10 mg prednisolone for ≥ 7 d) and/or other immunosuppressive therapies (2% (14 of 585)) including tacrolimus, methotrexate, cyclosporine and mycophenolate mofetil.

Table 1 | Clinical and oncological characteristics of 585 vaccinated patients with cancer

Cohort characteristics, <i>n</i> = 585	<i>n</i> (%)
Age, median (IQR), years	60 (52–68)
Male	323 (60)
Ethnicity, white	510 (87)
Previous SARS-CoV-2 infection and COVID-19 vaccination	<i>n</i> (%)
Previous SARS-CoV-2 infection^a	
Any test positive	181 (31)
RT-PCR positive	82 (14)
Serology positive	149 (25)
First COVID-19 vaccine	
AstraZeneca	430 (74)
Pfizer	153 (26)
Unknown	2 (0)
Time to second vaccine, median (IQR), d	77 (72–78)
Second COVID-19 vaccine	
AstraZeneca	402 (69)
Pfizer	142 (24)
Unknown	2 (0)
Reason for no second vaccine	
Death	16 (3)
Withdrew or lost to follow-up	10 (2)
Clinical advice	7 (1)
Patient choice	6 (1)
Oncological history	<i>n</i> (%)
Cancer type	
Solid, <i>n</i> = 447	
Stages I–II	55 (12)
Stage III	85 (19)
Stage IV	306 (68)
NA	1 (0)
Hematological	138 (24)
Concomitant medications^b within 48 h of vaccination	

Continued

Table 1 | Clinical and oncological characteristics of 585 vaccinated patients with cancer (Continued)

Cohort characteristics, <i>n</i> = 585	<i>n</i> (%)
Corticosteroids, >10 mg prednisolone equivalent	29 (5)
G-CSF	12 (3)
Other immunosuppression	14 (2)
Cyclosporin	6 (1)
Mycophenolate mofetil	6 (1)
Methotrexate	1 (0)
Tacrolimus	1 (0)
Solid cancers, <i>n</i> = 447	<i>n</i> (%)
Diagnosis	
Genitourinary	93 (21)
Skin	91 (20)
Gastrointestinal	87 (19)
Thoracic	63 (14)
Breast	52 (12)
Gynecological	27 (6)
Head and neck	13 (3)
Other	21 (5)
Disease status (with respect to last intervention)	
SACT, palliative	
CR	32 (7)
PR	80 (18)
SD	116 (26)
PD	86 (19)
Unknown	1 (0)
SACT, neoadjuvant or radical CRT	
CR, PR or SD	24 (5)
PD	1 (0)
Unknown	1 (0)
Surgery	
NED, adjuvant SACT	74 (17)
NED, surgery alone	17 (4)
Untreated and/or active surveillance	15 (3)
Recent anticancer treatment^c	
Systemic therapy	
Chemotherapy, <28 d	104 (23)
Targeted therapy, <28 d	145 (32)
Anti-PD-(L)1 ± anti-CTLA4, <183 d	109 (24)
Endocrine therapy, <28 d	20 (4)
No SACT, <28 d; no CPI, <112 d	145 (32)
Local therapy	
Surgery, <28 d	12 (3)
Radiotherapy, <28 d	20 (4)
Active IRAEs, secondary to CPI	38 (9)
Hematological malignancies, <i>n</i> = 138	<i>n</i> (%)
Diagnosis	
Lymphoma	53 (38)
Myeloma	36 (26)

Continued

Table 1 | Clinical and oncological characteristics of 585 vaccinated patients with cancer (Continued)

Cohort characteristics, n = 585	n (%)
Acute leukemia	25 (18)
CLL	16 (12)
MDS and MPN	7 (5)
Aplastic anemia	1 (1)
Disease status	
MRD or CR	72 (52)
Partial remission	34 (25)
SD	5 (4)
PD, relapse or untreated acute presentation	27 (20)
Anticancer treatment	
Chemotherapy, <28 d	19 (14)
Targeted therapy, <28 d	55 (40)
Anti-CD20 therapy, <12 months	26 (19)
CAR-T, <6 months	3 (2)
No SACT, <28 d; no SCT or anti-CD20, <12 months	64 (46)
Hematologic stem cell transplant	
Any previous stem cell transplant	58 (39)
Time from transplant, median (IQR), d	855 (215–1,602)
Allograft, <6 months	7 (5)
Autograft, <6 months	2 (1)
GVHD ongoing at first vaccination	18 (13)
Non-oncological medical history	n (%)
Past medical history	
No PMHx	188 (32)
Obesity, BMI > 30	130 (22)
HTN	121 (21)
Diabetes melitus	54 (9)
Inflammatory or autoimmune	38 (6)
PVD, IHD or CVD	32 (5)
Previous history of cancer	63 (11)

^aAs some patients did not seroconvert following previous infection, our laboratory definition of previous SARS-CoV-2 was determined by either previous PCR and/or standard of care or laboratory anti-S1 IgG ELISA (Methods), and some patients tested positive in more than one modality. ^bSignificant corticosteroid exposure was >10 mg prednisolone for a duration of at least 7 d and given within 48 h of vaccination. Significant G-CSF exposure was within 48 h of vaccination or within 5 d if a pegylated preparation was used. ^cSACT was considered within 28 d of the last administration with the exception of CPI, for which treatment within 183 d was considered given prolonged receptor occupancy following administration¹⁹. BMI, body mass index; CAR-T, chimeric antigen receptor T cell; CTLA4, cytotoxic T lymphocyte-associated protein 4; CR, complete response; CRT, chemoradiation; CVD, cerebrovascular disease; GVHD, graft-versus-host disease; HTN, hypertension; IRAE, immune-related adverse event secondary to CPI therapy; IHD, ischemic heart disease; MPN, myeloproliferative neoplasm; MRD, minimal residual disease; NA, not available; NED, no evidence of disease; PD, progressive disease; PD-(L)1, programmed cell death (ligand) 1; PMHx, past medical history; PR, partial response; PVD, peripheral vascular disease; SCT, stem-cell transplant; SD, stable disease.

Seroconversion rates following COVID-19 vaccine administration. Seroconversion (that is, the presence of S1-reactive antibodies) was assessed in infection-naive patients (defined as no history of COVID-19, tested negative for SARS-CoV-2 by RT-PCR and tested negative for S1-reactive antibodies before vaccination) at baseline, 2–4 weeks after the first vaccine dose and 2–4 weeks after the second vaccine dose (Fig. 1a). Due to the uncertainty of the effect of the extended 12-week dosing interval, we incorporated an additional sampling time point just before the second vaccine dose (Fig. 1a).

After the first dose, the seroconversion rate was 39% (Fig. 1b), with lower rates in patients with hematological malignancies (27%) than in those with solid malignancies (44%) (Fig. 1c). After the second dose, this increased to 78%, again with lower rates for hematological malignancies (59%) than for solid malignancies (85%) (Fig. 1b,c). Seroconversion rates were maintained during the 12-week dosing interval, with a nominal increase in the number of seroconverted patients immediately before the second dose relative to that at the earlier time point of 2–4 weeks (especially in those with hematological malignancies) (Fig. 1b,c).

NAb responses following COVID-19 vaccine administration. Functional humoral responses after vaccination were assessed in all patients using a high-throughput live virus-neutralization assay (Methods) against WT SARS-CoV-2 and the Alpha (B.1.1.7), Beta (B.1.351) and Delta (B.1.617.2) VOC and expressed as titers (representing the reciprocal of serum required to inhibit 50% of viral replication (IC₅₀)). The distribution of NAbT was categorized as undetectable (<40), moderate (40–256) and high (>256) as described in previously published reports using the same neutralization assay^{28–30}.

After the first dose, 49% of infection-naive patients had detectable NAb to WT SARS-CoV-2, with a significantly lower proportion having detectable NAb to VOC (Alpha, 15%; Beta, 9%; Delta, 9%) (Fig. 2a); the median NAbT were below the limit of detection for all strains (Fig. 2b). After the second dose, the proportion of patients with detectable NAbT against all strains increased but less so against VOC than against WT SARS-CoV-2 (WT, 83%; Alpha, 61%; Beta, 53%; Delta, 54%; χ^2 test, P value < 2.2×10^{-16}); the median NAbT also increased for all strains, again to a lesser extent for VOC than for WT SARS-CoV-2 (Fig. 2a,b).

We observed that NAbT against Delta, but not against WT, Alpha or Beta, were significantly higher in infection-naive patients who received two vaccine doses than those in vaccine-naive patients who recovered from SARS-CoV-2 (WT or Alpha) infection (Fig. 3a). Among those with prior SARS-CoV-2 infection, the proportion of patients with NAb against WT SARS-CoV-2 increased from 62% at baseline to 85% after the first vaccine dose and to 95% after the second vaccine dose (the corresponding proportions for Alpha were 52%, 65% and 88%; Beta, 39%, 61% and 80%; Delta, 41%, 59% and 80%). After the first and second doses, patients with prior SARS-CoV-2 infection had significantly higher median NAbT than infection-naive patients (WT, 15 fold after the first dose and fourfold after the second dose; Alpha, tenfold and fivefold; Beta, threefold and fourfold; Delta, threefold and fourfold) (Fig. 3b).

We next analyzed the NAb response by vaccine type. In SARS-CoV-2 infection-naive patients, there were no significant differences in the proportion of patients with detectable NAb by vaccine type after the first dose (AZ, 54% (WT), 16% (Alpha), 10% (Beta), 10% (Delta); PZ, 30% (WT), 9% (Alpha), 7% (Beta), 5% (Delta)), with higher median NAbT observed with AZ than those with PZ against WT SARS-CoV-2 but not VOC (Fig. 3c). After the second dose, there were significant differences in the proportion of patients with detectable NAb by vaccine type (AZ, 85% (WT), 59% (Alpha), 49% (Beta), 50% (Delta); PZ, 78% (WT), 68% (Alpha), 64% (Beta), 68% (Delta)), with significantly lower median NAbT observed with AZ than those with PZ against all variants (Fig. 3c). In patients with previous SARS-CoV-2 infection, there were no differences in the proportion with detectable NAb after the second dose (AZ, 96% (WT), 88% (Alpha), 78% (Beta), 79% (Delta); PZ, 92% (WT), 86% (Alpha), 83% (Beta), 81% (Delta)) or median NAbT after the first dose against all variants nor those after the second dose against WT, Alpha and Beta VOC. However, after the second dose, NAbT against Delta were significantly higher with PZ than those with AZ (Fig. 3d).

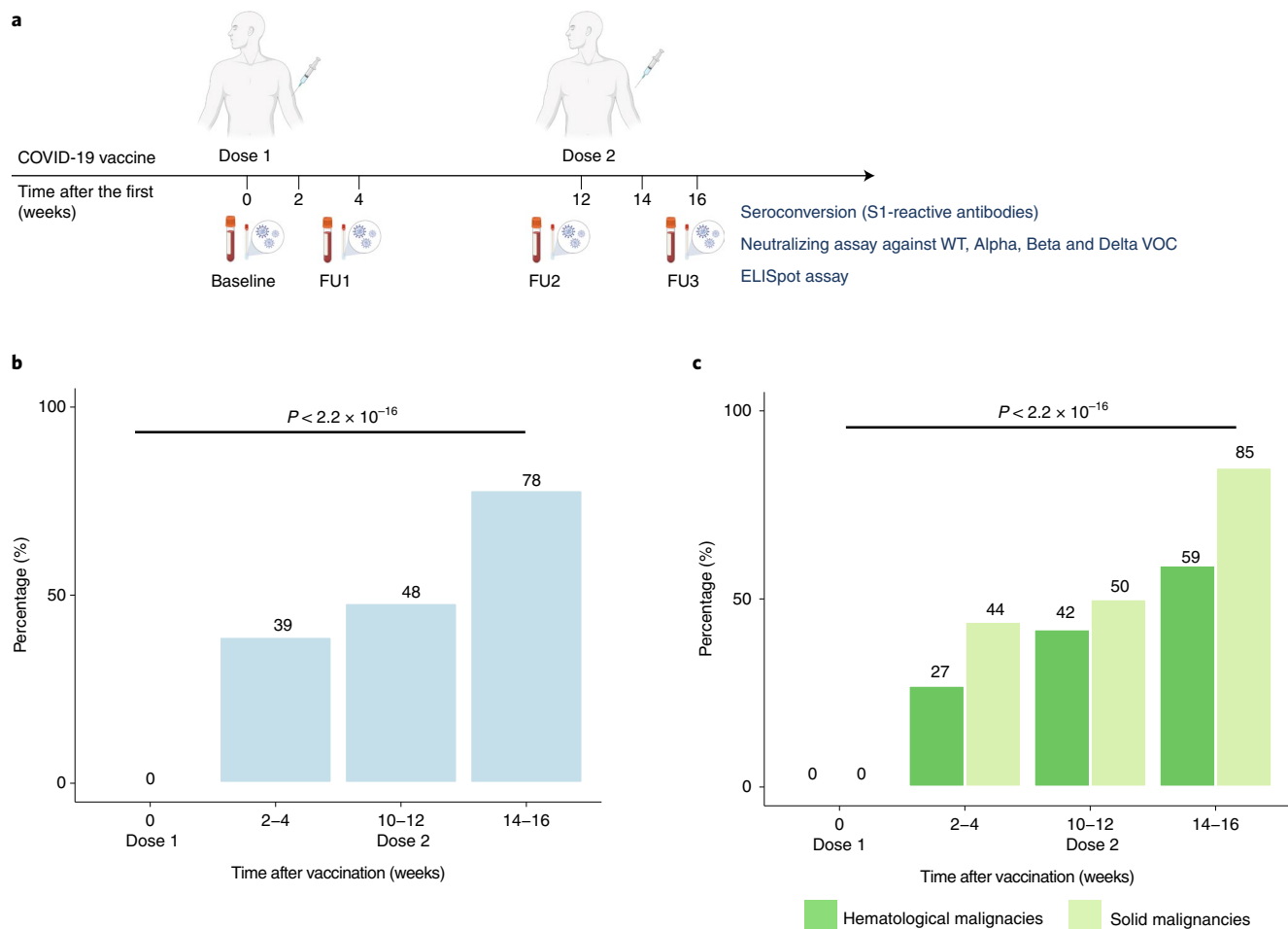


Fig. 1 | Seroconversion in patients with cancer after COVID-19 vaccination. **a**, Sampling and analysis schema in the CAPTURE study. Baseline samples were collected immediately before the first dose. Follow-up samples were collected 2–4 weeks after the first dose (follow-up (FU)1), on the day of and immediately before the second dose (FU2; that is, the additional time point after the first dose implemented due to the delayed 12-week dosing interval) and 2–4 weeks after the second dose (FU3). S1-reactive antibody tests (that is, seroconversion) and NAb assays were performed in all available follow-up samples from 585 patients. **b**, Proportion of infection-naïve patients ($n=328$, 323, 256 and 312 patients at baseline, FU1, FU2 and FU3, respectively) with S1-reactive antibodies at each time point. Differences were analyzed using the χ^2 test. P values < 0.05 were considered significant. **c**, Proportion of infection-naïve patients with S1-reactive antibodies grouped by solid ($n=270$, 234, 192 and 234 patients at baseline, FU1, FU2 and FU3, respectively) and hematological malignancies ($n=58$, 89, 64 and 78 patients at baseline, FU1, FU2 and FU3, respectively). Differences were analyzed by the χ^2 test. P values < 0.05 were considered significant. FU1, 21–56 d after the first vaccine; FU2, 14–28 d before the second vaccine; FU3, 14–28 d after the second vaccine.

NAb against VOC and S1-reactive antibodies show discordance.

To understand the ability of the S1-reactive antibody assay (detecting IgG antibodies specific to WT SARS-CoV-2) to predict functional humoral immunity against currently circulating VOC, we analyzed per-patient agreement of seroconversion and detectable NAb. We observed good concordance between the presence of S1-reactive antibodies and NAb against the WT strain. However, there was discordance in the case of VOC; for example, 55% of patients without detectable NAb against Delta had detectable anti-S1 IgG antibodies following two vaccine doses (Supplementary Table 4).

Impact of prior infection and cancer subtypes on the NAb response.

Among infection-naïve patients with solid cancers ($n=308$) after the first dose, 58% had detectable NAb against WT SARS-CoV-2, 17% had NAb against Alpha, 11% had NAb against Beta and 12% had NAb against Delta. After the second dose, this increased to 92% of patients with detectable NAb against WT, 70% of patients with NAb against Alpha, 61% of patients with NAb against Beta and 62% of patients with NAb against Delta. However, in infection-naïve patients with hematological malignancies

($n=96$), proportions were lower both after the first dose (25%, WT; 7%, Alpha; 5%, Beta; 1%, Delta) and after the second dose (56%, WT; 35%, Alpha; 28%, Beta; 31%, Delta). Furthermore, median NAbT against all strains were significantly lower in patients with hematological malignancies than those in patients with solid cancers, especially after the second dose (Fig. 2c). For both solid and hematological malignancies, the proportion of patients with detectable NAbT and median NAbT were significantly higher in those with previous infection than those in infection-naïve patients at baseline and after the first and second vaccine dose; although, again, values were lower for those with hematological malignancies than for those with solid cancers (Extended Data Fig. 2a,b). Specifically, after the second dose, NAb against WT were detectable in 80% of patients with hematological malignancies (70%, Alpha; 60%, Beta; 57%, Delta) and in 99% of patients with solid cancers (92%, Alpha; 80%, Beta; 86%, Delta).

Patients with hematological malignancies had a range of responses toward WT SARS-CoV-2. For example, following two vaccine doses, a higher proportion of patients with multiple myeloma had detectable NAb (WT, 89%; Alpha, 53%; Beta, 21%;

Delta, 32%) than those with chronic lymphocytic leukemia (CLL) (WT, 20%; Alpha, 0%; Beta, 10%; Delta, 20%) with accordingly varied median NAbT against WT (multiple myeloma, 131; CLL, <40), although not against VOC (Extended Data Fig. 3a). By contrast, in patients with solid cancers, there were no significant differences in the NAb response against any variant after the second dose according to cancer subtype (Extended Data Fig. 3b).

Impact of clinical and treatment characteristics on the NAb response. We next used ordinal regression models to assess which patient and cancer characteristics (including systemic anticancer therapy (SACT)) associate with NAbT (categorized as undetectable (<40), moderate (40–256) and high (>256)). Considering all patients, lack of previous SARS-CoV-2 infection, the AZ vaccine, older age and hematological malignancy but not sex or comorbidities were associated with reduced NAbT to SARS-CoV-2 WT and VOC both after the first dose and after the second dose (Supplementary Table 5).

Considering hematological malignancies alone, regression analysis confirmed the previously observed association of hematological malignancy subtype with lower NAbT against WT SARS-CoV-2 (but not VOC) (Supplementary Table 6). Further, anti-CD20 treatment ≤ 12 months before vaccination was associated with reduced NAbT against SARS-CoV-2 WT and VOC after first and second vaccine doses (Extended Data Fig. 4a). There was no significant association between vaccine type and NAbT, but lack of previous infection and older age were significantly associated with reduced NAbT against all variants (Supplementary Table 6).

Considering solid cancers alone, no significant associations with reduced NAbT were found (including cancer subtype and stage, SACT and disease status after SACT) beyond the lack of previous infection, older age and the AZ vaccine (Supplementary Table 7).

Finally, we did not observe any detrimental effects of granulocyte colony-stimulating factor (G-CSF), corticosteroids or immunosuppressive therapy (including active graft-versus-host in patients with hematological malignancies) on NAbT against any SARS-CoV-2 strain in patients with solid or hematological malignancies (Supplementary Tables 6 and 7).

Comparison of NAb responses with individuals without cancer. Next, we compared NAbT induced by vaccination between patients with cancer in the CAPTURE study and healthy participants in the Legacy study^{28,29}. Critically, the same neutralizing assays were applied in both cohorts. Overall, following two vaccine doses, NAbT against WT were detectable in 100% of healthy Legacy participants (Alpha, 96%; Beta, 86%; Delta, 85%) as compared to in 87% of CAPTURE patients with cancer (Alpha, 70%; Beta, 62%; Delta, 63%). Of note, individuals recruited to the Legacy study were considerably younger and more frequently received the PZ vaccine. We therefore matched CAPTURE and Legacy participants by factors that impact NAbT

(Methods), including vaccine type, previous infection and age. Due to the heterogeneity between the two cohorts, matching resulted in attrition of individuals available for comparison.

We first assessed infection-naïve individuals vaccinated with PZ. The proportion of patients with solid cancer ($n=49$) who had detectable NAbT after the second dose was only numerically lower than that of individuals without cancer ($n=55$) (WT, 98% versus 100%; Alpha, 92% versus 100%; Beta, 86% versus 91%; Delta, 92% versus 95%, respectively) (Extended Data Fig. 5a), and the two groups had comparable median NAbT against all variants (Extended Data Fig. 5b). However, a significantly lower proportion of patients with hematological malignancies ($n=24$) than individuals without cancer had detectable NAbT (WT, 37%; Alpha, 17%; Beta, 17%; Delta, 17%) (Extended Data Fig. 5a), with significantly lower median NAbT against all variants (Extended Data Fig. 5b). We note that patients with hematological malignancies vaccinated with PZ were more likely to have CLL or lymphoma and treatment with anti-CD20 therapy than patients vaccinated with AZ.

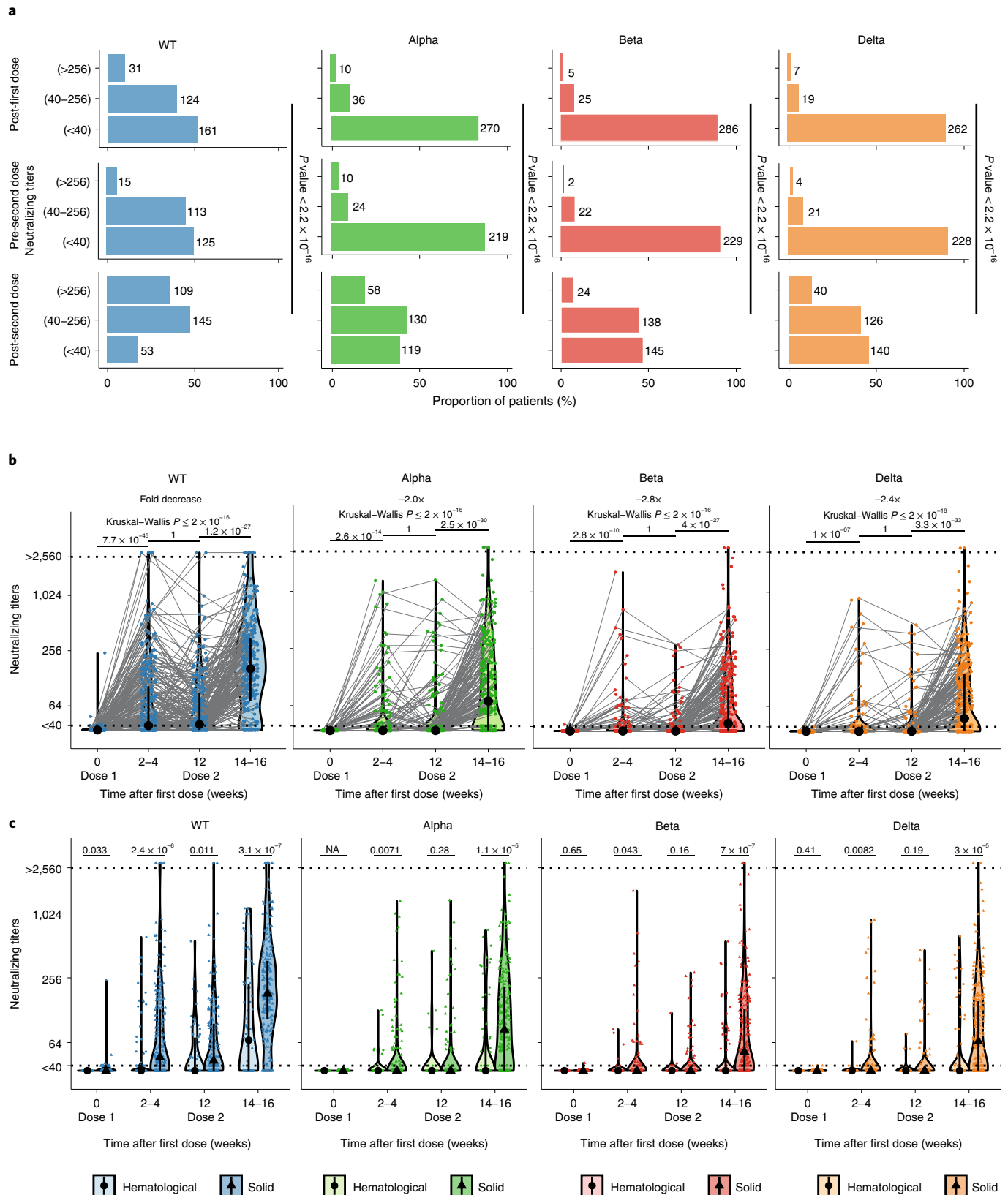
Only a small number of age-matched Legacy participants received the AZ vaccine ($n=8$ infection-naïve patients, aged 40–59 years). After the second dose, a numerically lower proportion of patients with solid cancers ($n=77$) had detectable NAbT against all variants other than Delta than individuals without cancer (WT, 92% versus 100%; Alpha, 66% versus 75%; Beta, 60% versus 75%; Delta, 60% versus 50%, respectively) (Extended Data Fig. 5c), but this was not statistically significant, and median NAbT were comparable (Extended Data Fig. 5d). As with PZ, a lower proportion of patients with hematological malignancies ($n=18$) than those without cancer had detectable NAbT against all variants (WT, 73%; Alpha, 40%; Beta, 20%; Delta, 36%), with correspondingly lower NAbT (Extended Data Fig. 5c,d). We note that patients vaccinated with AZ with hematological malignancies were more likely to have acute leukemia (ALL) or myeloma and were less likely to have received anti-CD20 therapy than patients vaccinated with PZ.

COVID-19 vaccines induce T cell responses in patients with cancer. We evaluated S-specific T cell responses following one or two vaccine doses (Supplementary Table 3) by interferon (IFN)- γ enzyme-linked immunospot (ELISpot) after stimulation with WT or Alpha S peptide pools in a subset of 337 patients with cancer (Methods, Fig. 4a and Extended Data Fig. 1b,c). For 13 of 337 patients (4%, ten with solid cancer and three with hematological malignancies), all samples were excluded either due to low viable cell count or a failed negative or positive control in the assay. Of the 324 remaining patients, 279 had solid cancer (of whom 94% had NAb against WT, 77% had NAb against Alpha, 73% had NAb against Beta and 71% had NAb against Delta) and 58 had hematological malignancies (of whom 69% had NAb against WT, 49% had NAb against Alpha, 39% had NAb against Beta and 45% had NAb against Delta). Delta S peptide pools were analyzed in a subset of 86 patients with cancer.

Fig. 2 | NAb against WT SARS-CoV-2 and VOC. **a**, NAbT in infection-naïve patients were categorized as undetectable or low (<40), medium (40–256) or high (>256) and are shown for WT SARS-CoV-2 and the three VOC. Differences were analyzed using the χ^2 test. P values < 0.05 were considered significant. Numbers in the panel indicate sample numbers. **b**, NAbT in infection-naïve patients against WT SARS-CoV-2 and the Alpha, Beta and Delta VOC. Median fold decrease in NAbT is shown for each VOC in comparison with that for WT SARS-CoV-2 ($n=318, 316, 253$ and 307 patients at baseline, FU1, FU2 and FU3, respectively). The dotted line at <40 denotes the lower limit of detection; the dotted line at >2,560 denotes the upper limit of detection. Violin plots denote density of data points. The point range denotes the median and the 25th and 75th percentiles. Dots represent individual samples. Samples from individual patients are connected. Significance was tested by Kruskal-Wallis test; $P < 0.05$ was considered significant; for the post hoc test, a two-sided Mann-Whitney U -test with Bonferroni correction was used for pairwise comparisons. Only comparisons with the prior time point are denoted in the graph. **c**, Comparison of NAbT in infection-naïve patients with solid ($n=262, 232, 189$ and 232 patients at baseline, FU1, FU2 and FU3, respectively) versus hematological malignancies ($n=56, 84, 64$ and 75 patients at baseline, FU1, FU2 and FU3, respectively). The dotted line at <40 denotes the lower limit of detection; the dotted line at >2,560 denotes the upper limit of detection. Violin plots denote density of data points. The point range denotes the median and the 25th and 75th percentiles. Dots represent individual samples. Significance was tested by two-sided Wilcoxon-Mann-Whitney U -test; $P < 0.05$ was considered significant. NA, not tested.

In infection-naïve patients, T cell responses to WT S peptide pools were detected in 22% of patients at baseline, suggesting cross-reactivity to other human coronaviruses (companion paper²⁷). After the first vaccine dose, 44% of evaluated patients had a detectable T cell response to WT S peptide pools (that is, >24 spot-forming units (SFU) per

10⁶ peripheral blood mononuclear cells (PBMCs), Methods), which increased to 56% immediately before the second dose and to 79% after the second dose. SFU levels increased significantly both after the first dose and after the second dose (median 3.3-fold and 13-fold increase versus baseline levels, respectively; Fig. 4b).



Regarding patients with prior SARS-CoV-2 infection, 32% had detectable T cell responses to WT S peptide pools at baseline, which increased to 69% after the first dose and 87% after the second dose. Median levels of SFU specific to the WT S protein were significantly higher than those in infection-naïve patients at baseline. To confirm that increased baseline T cell responses were related to previous infection, we also measured responses after stimulation with nucleocapsid (N) and membrane (M) peptide pools and found that median SFU levels were higher at baseline in those with previous infection (Extended Data Fig. 6a). Furthermore, we observed a significant increase in numbers of SFU against the Alpha VOC but not against the Delta VOC after the second vaccine dose, independent of infection status (Extended Data Fig. 6b,c).

The proportion of infection-naïve patients with hematological malignancies who had T cell responses to WT S peptide pools was only nominally different from that of those with solid cancers (34% versus 45% after the first dose and 83% versus 78% after the second dose) (Fig. 4d). While SFU numbers were significantly lower in patients with hematological malignancies than in those with solid cancers after the second dose (median SFU per 10^6 PBMCs, 50.5 versus 98.3), in a logistic regression model, there was no significant association between detectable T cell responses and cancer type, patient characteristics or vaccine type (AZ or PZ) (Fig. 4e and Extended Data Fig. 6d). There were no significant differences in SFU numbers between cancer subtypes after the second dose (Fig. 4f). In addition, we detected T cell responses after two vaccine doses in four of four evaluated patients treated with anti-CD20 therapy (Extended Data Fig. 6e). Consistent with type 1 helper T (T_H1) cell responses, we detected increased concentrations of tumor necrosis factor (TNF), interleukin (IL)-2, IL-18, IL-12 p40 and IFN- γ -induced protein (IP)-10 after stimulation with S1 or S2 peptide pools compared to those in unstimulated controls (Extended Data Fig. 6f), with comparable levels of these cytokines in patients with hematological ($n=25$) and solid cancers ($n=8$) (Extended Data Fig. 6g). Finally, SFU levels and the proportion of patients with detectable S-reactive T cells (solid, 77%; hematological, 80%) after two vaccine doses were not significantly different than those in healthcare worker controls (80%, $n=25$) (Supplementary Table 8 and Extended Data Fig. 7).

We also observed T cell responses in patients without detectable NAb (Supplementary Table 9). For example, in patients with hematological malignancies, T cell responses were detected in 92% of patients (11 of 12) without detectable NAb against WT SARS-CoV-2 (in 80% of patients without NAbT against Alpha, 75% of patients without NAbT against Beta and 86% of patients without NAbT against Delta).

SARS-CoV-2 infection in vaccinated patients with cancer. At the time of database lock (median of 55 d after the second vaccine dose), 1% of patients (8 of 585; 4 patients with AZ, 4 patients with PZ) had tested positive for SARS-CoV-2 by RT-PCR, with six patients testing positive between the first and second dose and two patients

testing positive after the second vaccine dose (Extended Data Fig. 8). Three patients had a diagnosis of hematological cancer, and five patients were diagnosed with solid malignancies. Three patients had evidence of past SARS-CoV-2 infection at the time of the first vaccine dose (minimum of 30 d since previous positive SARS-CoV-2 RT-PCR test).

Overall, five of eight patients were identified through routine screening (World Health Organization (WHO) severity score of 1)³¹, of whom four were asymptomatic and one subsequently developed fever and anosmia (WHO severity score of 2). Three patients presented with symptoms (WHO severity score of 3–5) (Extended Data Fig. 8).

For technical reasons, we were only able to confirm lineage by viral genome sequencing in one patient (Alpha); but, given the timing of presentation, these patients were likely infected with either Alpha or Delta VOC. At the last evaluable time point before infection, six of eight patients had detectable NAb to WT SARS-CoV-2, but fewer had detectable NAb to VOC (four of eight, Alpha; four of eight, Beta; four of eight, Delta) with correspondingly lower NAbT. The patient with the most severe disease course (CV0217, Extended Data Fig. 8) presenting after the first vaccine dose had no evidence of NAb to SARS-CoV-2 WT or VOC after the first or second vaccine dose or at any time during the course of COVID-19 illness. SARS-CoV-2-specific T cells were only detectable in one of four patients before infection and after the first vaccine dose.

Discussion

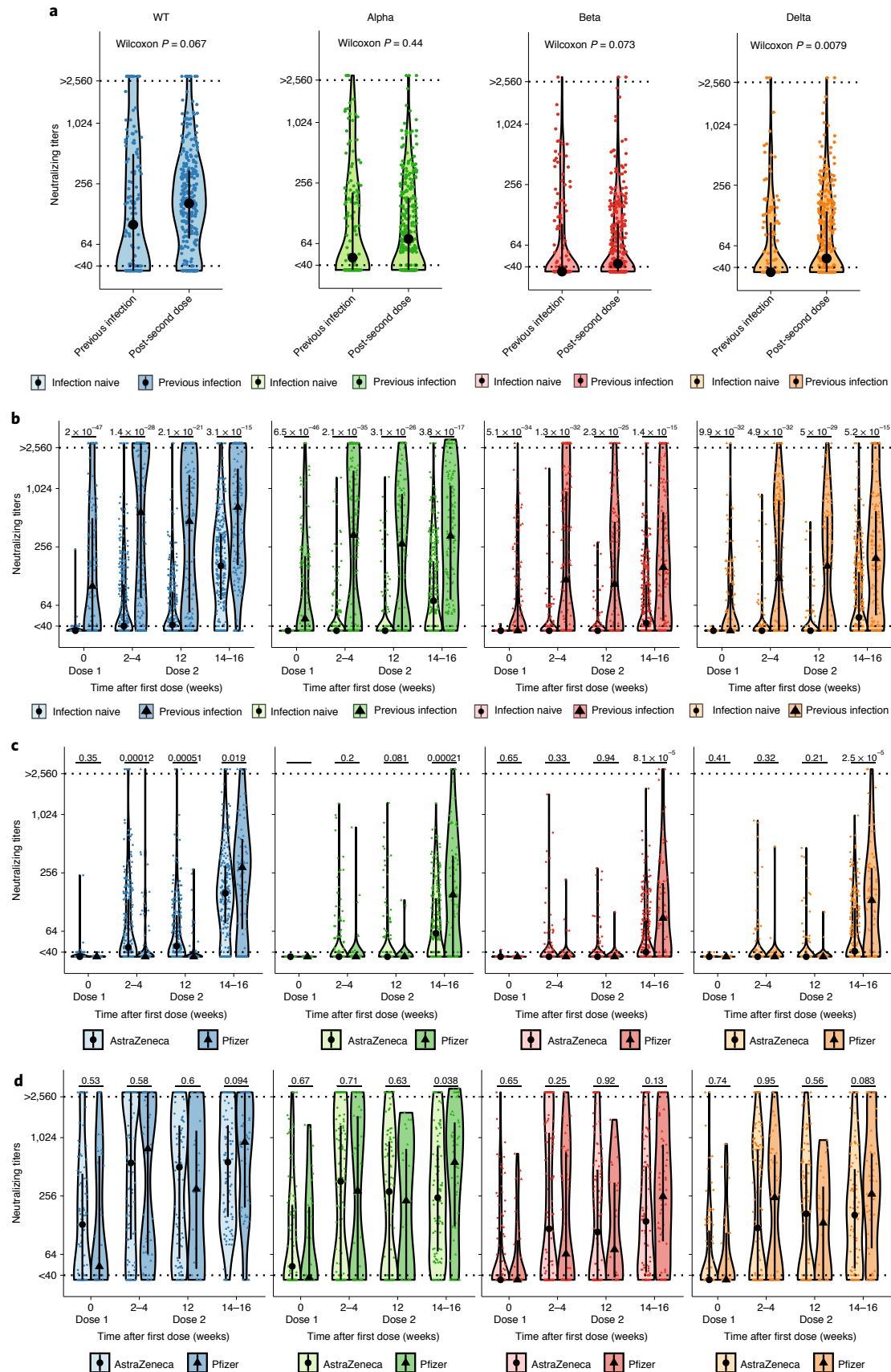
Our prospective study of 585 patients with cancer following AZ or PZ COVID-19 vaccination revealed an overall 78% seroconversion rate, with lower rates in patients with hematological malignancies (59%) than in those with solid malignancies (85%). This was numerically comparable to results in other studies in patients with cancer^{15–17,24,32,33} and lower than rates in the general population (99%)³⁴. Importantly, functionally relevant NAb against Delta were detectable in only 54% of infection-naïve patients with cancer (62% and 31% in solid and hematological malignancies, respectively; 50% and 68% with AZ and PZ, respectively), lower than the reported 85% using the same neutralization assay in a younger population without cancer^{28,29}.

Given the complete dominance of Delta in the UK and its surging prevalence globally, our data on NAb activity against VOC have contemporary implications for the care of patients with cancer who are at increased risk of adverse outcomes of SARS-CoV-2 infection. Studies in patients with cancer to date have used seroconversion (that is, detection of IgG antibodies against the WT S protein) as the main immunogenicity endpoint^{14–24,32}, but NAb against VOC have not been evaluated. Although we found good concordance between the presence of anti-S1 IgG antibodies and NAbT against WT SARS-CoV-2 in our cohort (in line with reports on those without cancer)^{35–37}, seroconversion was a poorer surrogate for NAbT against VOC, for which approximately half of patients without detectable NAb against Delta had anti-S1 IgG antibodies. The

Fig. 3 | Neutralizing response against WT SARS-CoV-2 and VOC by prior SARS-CoV-2 infection status and type of COVID-19 vaccine. **a**, Comparison of NAbT against WT SARS-CoV-2, Alpha, Beta and Delta in patients with previous infection before vaccination as compared to infection-naïve patients after the second dose ($n=133$ and 306 patients at baseline and FU3, respectively). Significance was tested by two-sided Wilcoxon–Mann–Whitney U -test; $P < 0.05$ was considered significant. **b**, Comparison of NAbT against WT SARS-CoV-2, Alpha, Beta and Delta in infection-naïve patients ($n=318$, 316 , 253 and 307 patients at baseline, FU1, FU2 and FU3, respectively) versus patients previously infected with SARS-CoV-2 ($n=133$, 163 , 115 and 144 patients at baseline, FU1, FU2 and FU3). Comparison of NAbT against WT SARS-CoV-2, Alpha, Beta and Delta in infection-naïve patients receiving AZ ($n=262$, 246 , 212 and 229 patients at baseline, FU1, FU2 and FU3, respectively) versus those receiving PZ ($n=56$, 70 , 41 and 77 patients at baseline, FU1, FU2 and FU3, respectively; one patient with unknown vaccine status was not included) (**c**) and in patients with previous SARS-CoV-2 infection receiving AZ ($n=99$, 117 , 92 and 91 patients at baseline, FU1, FU2 and FU3, respectively) versus those receiving PZ ($n=34$, 46 , 23 and 53 patients at baseline, FU1, FU2 and FU3, respectively) (**d**). The dotted line at <40 denotes the lower limit of detection; the dotted line at $>2,560$ denotes the upper limit of detection. Violin plots denote density of data points. The point range denotes the median and the 25th and 75th percentiles. Dots represent individual samples. Significance in **b–d** was tested by two-sided Wilcoxon–Mann–Whitney U -test; $P < 0.05$ was considered significant.

recombinant S1 protein used in the serological assay corresponds to the WT sequence, and selection of spike mutations in VOC leads to diminished neutralizing activity of such antibodies. Given that

NAb are highly predictive of immune protection from symptomatic SARS-CoV-2 infection^{35,38,39}, our data suggest that serological assays may underestimate the risk of breakthrough infection when



not accounting for viral evolution and the disconnect with NAbT against VOC.

An inverse relationship between age and vaccine-induced neutralizing responses was recently shown in individuals without cancer, with those aged >80 years particularly affected⁴⁰. Likewise, in our cohort of patients with cancer, increasing age correlated with reduced NAbT. The unmatched comparison of CAPTURE patients with cancer with the younger Legacy cohort (median age, 35.3 years) also showed reduced NAbT, further highlighting the effect of age on vaccine response. Given the relatively young median age in our cohort (60 years), it is possible that the effect of age in the general population with cancer is even more pronounced.

The mix of patients who received AZ or PZ vaccines, delivered 12 weeks apart as per current UK guidelines, uniquely facilitated assessment of differential responses to the two vaccines within a lengthened time frame. Despite maintained seroconversion rates between doses for either vaccine, the interval between first and second doses still represents an 'at-risk' period, during which neither vaccine led to a robust NAb response against VOC. After the first dose, NAbT against Delta were undetectable for 90% (AZ) and 95% (PZ) of patients, although NAbT against WT were higher with AZ than those with PZ. After the second dose, NAbT increased, but the levels were still diminished against VOC compared with those against SARS-CoV-2 WT. This was more pronounced with AZ than with PZ (50% versus 68% of infection-naive patients had detectable NAbT against Delta after two doses), consistent with the modestly reduced effectiveness of AZ (67%) as compared to PZ (88%) against Delta VOC in the general UK population⁴¹. The implications of our findings are twofold. First, a proportion of patients with cancer who are 'double vaccinated' may still be suboptimally protected when transmission rates of VOC in the community are high. Second, while broad debate remains on the optimal dosing schedule of two-dose regimens (by efficacy or resource-distribution arguments), our data suggest that a shorter interval (<12 weeks) between vaccine doses may minimize the 'at-risk' period for patients with cancer who do not develop NAb during the prolonged dosing schedule. A potential trade-off to this may be overall lower antibody titers with a shortened schedule^{42,43}, but this may conceivably be rescued with a third vaccine dose.

We note that differences in NAbT between individuals receiving AZ and PZ in our cohort, consistent with findings in patients on hemodialysis³⁰, are largely driven by patients with solid cancers. In patients with hematological malignancies, NAb responses were generally low without a discernible impact of the vaccine type. NAbT were lowest in patients treated with anti-CD20 antibodies, and patients with CLL were more likely to lack NAb than those with

multiple myeloma (Delta, 0% versus 32%, respectively). Irrespective of the underlying malignancy type, levels of NAb against VOC were augmented by prior SARS-CoV-2 infection with an incremental increase in seroconversion and NAbT following two vaccine doses. This suggests that patients with cancer, especially those with hematological malignancies, would benefit from a third vaccine dose to further boost humoral immunity. Two recent studies of solid organ-transplant recipients ($n=101$ (ref. ⁴⁴) and $n=120$ (ref. ⁴⁵)), in which the third dose significantly improved immunogenicity of the PZ vaccine, lend further support to this notion (although differences between infection and vaccination in antigen load and degree of T or B cell stimulation need to be acknowledged). Furthermore, recent data on the added benefits of heterologous vaccination regimens^{46–49} through boosting of both antibody and T cell responses may be especially relevant for patients with hematological malignancies who have lower NAb responses to both AZ and PZ. We also note a report of a patient with lymphoplasmacytic lymphoma treated with rituximab (anti-CD20 antibody) who failed to seroconvert after two doses of the PZ vaccine but developed NAb following a booster with JNJ-78436735 (Johnson & Johnson, a viral vector vaccine)⁵⁰. Prospective data are needed to determine the optimal vaccination regimen in immunocompromised patients.

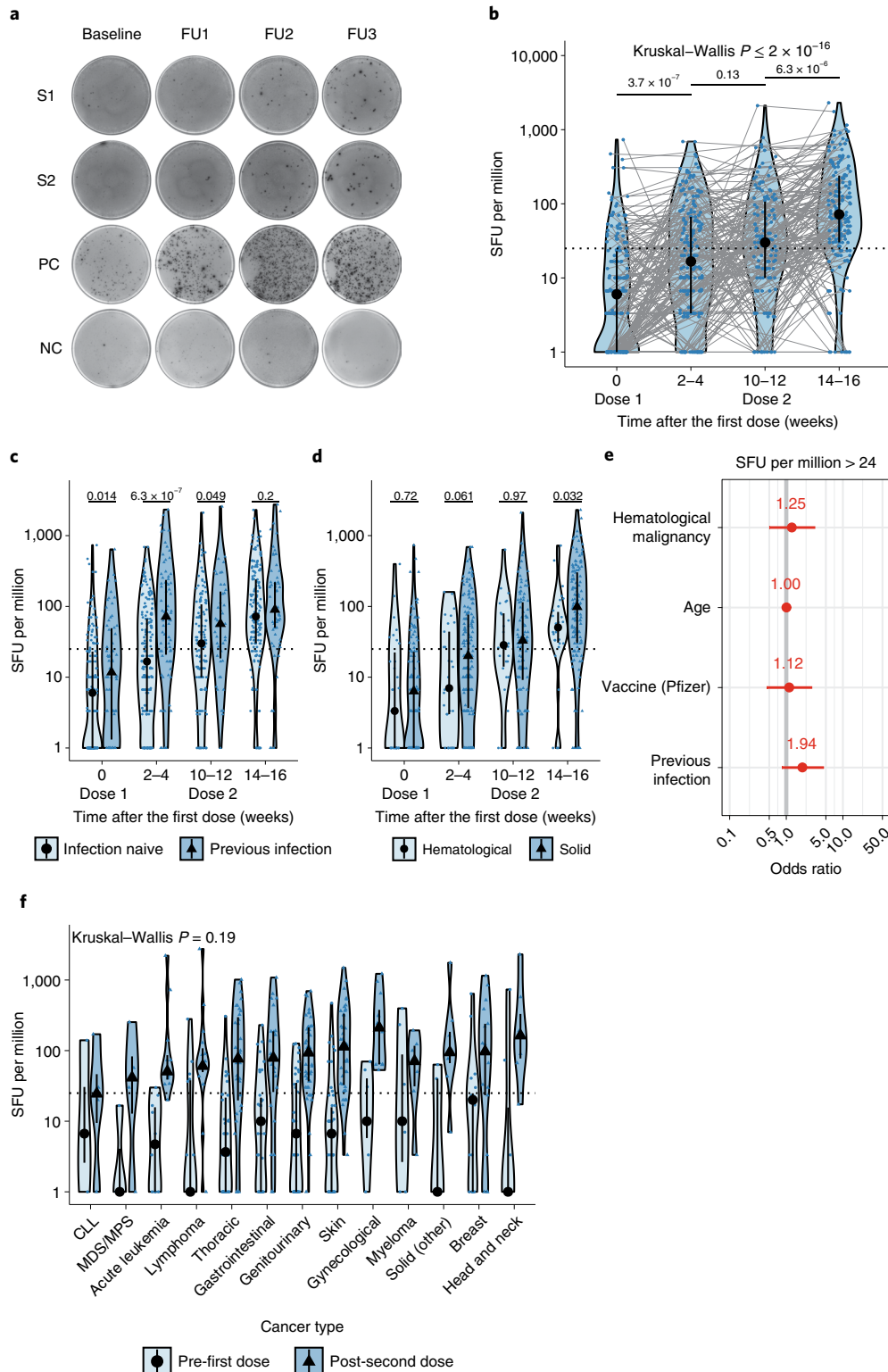
In the most substantial evaluation of cellular immunity to COVID-19 resulting from vaccination in patients with cancer to date ($n=324$), we observed SARS-CoV-2-specific T cell responses in the majority of patients, and responses occurred in a range similar to that of healthy individuals. Importantly, we detected T cell responses against Alpha and Delta peptide pools, in agreement with a recent report suggesting that T cells induced by WT SARS-CoV-2 were effective against VOC⁵¹. Critically, in our cohort, T cell responses were observed in most patients with hematological malignancies, including those with undetectable NAbT. Additionally, patients with solid and hematological malignancies had comparable T_H1-driven responses. The dissonance of humoral and cellular responses was also observed with SARS-CoV-2 infection (companion paper²⁷), including in patients on anti-CD20 therapy, suggesting that cellular immunity offers some immune protection in this patient group. Overall, however, our understanding of the role of T cells in immune protection from SARS-CoV-2 remains incomplete; while they are not expected to prevent infection, T cell responses are likely to reduce COVID-19 severity. Preclinical studies in mice⁵² and rhesus macaques⁵³ have demonstrated the role of cellular immunity in SARS-CoV-2 clearance. A study of patients with multiple sclerosis on anti-CD20 treatment ($n=20$) reported suppressed humoral responses but augmented CD8⁺ T cell induction and preserved T_H1 priming following COVID-19 vaccination⁵⁴.

Fig. 4 | WT SARS-CoV-2-specific T cell responses in patients with cancer following vaccination. **a**, Exemplar ELISpot illustrating WT SARS-CoV-2-specific T cell responses. PBMCs were stimulated with 15-mer peptide pools spanning the S1 or S2 subunit of the S protein. T cell responses represent the sum of SFU per 10⁶ PBMCs after stimulation with WT S1 or S2 peptide pools. NC, negative control; PC, positive control. **b**, SFU per 10⁶ PBMCs in infection-naive patients after vaccination ($n=165, 195, 122$ and 160 patients at baseline, FU1, FU2 and FU3, respectively). The dotted line at <24 denotes the threshold for positivity. Violin plots denote density; the point range shows the median and 25th and 75th percentiles. Dots represent individual samples. Samples from individual patients are connected. Significance was tested by Kruskal-Wallis test; for the post hoc test, two-sided Wilcoxon-Mann-Whitney *U*-test with Bonferroni correction was used. Only comparisons with the prior time point are denoted in the graph. Comparison of SFU per 10⁶ PBMCs in patients with ($n=70, 88, 49$ and 69 patients at baseline, FU1, FU2 and FU3, respectively) and without prior SARS-CoV-2 infection ($n=165, 195, 122$ and 160 patients at baseline, FU1, FU2 and FU3, respectively) (**c**) and in patients with solid ($n=136, 161, 98$ and 130 patients at baseline, FU1, FU2 and FU3, respectively) versus hematological malignancies ($n=29, 34, 24$ and 30 patients at baseline, FU1, FU2 and FU3, respectively) (**d**). Violin plots denote density; the point range shows the median and 25th and 75th percentiles. Dots represent individual samples. Significance in **c-d** was tested by two-sided Wilcoxon-Mann-Whitney *U*-test. **e**, Binary logistic regression of SFU per million PBMCs in patients with solid tumors versus those with hematological malignancies. Dots denote odds ratios (blue, positive odds ratio; red, negative odds ratio); whiskers denote IQR $\times 1.5$. **f**, Comparison of SFU per million PBMCs in patients with hematological malignancies and solid tumors before the first dose and after the second dose. The dotted line at <24 denotes the lower limit of detection. Violin plots denote density. The point range denotes the median and the 25th and 75th percentiles. Dots represent individual samples. Significance was tested by Kruskal-Wallis test; $P < 0.05$ was considered significant; for the post hoc test, two-sided Wilcoxon-Mann-Whitney *U*-test with Bonferroni correction was used. MDS, myelodysplastic syndrome.

Overall, the absolute excess risk for post-vaccination breakthrough infection with skewed immunity toward a cellular response is unquantified.

Among patients with solid malignancy, cancer subtype impacted neither NAbT nor T cell responses to vaccination. Of note, in patients with thoracic malignancies who are known to be at higher risk of severe outcomes of COVID-19 (refs. 8,11,55,56), vaccine-induced immunity was not inferior as compared to that in patients with other solid cancers. Furthermore, systemic therapy, including CPI

and corticosteroids, were not detrimental to induction of immune response to vaccination. This is reassuring and further reflected by the finding that median NAbT among PZ-vaccinated patients with solid cancers were comparable to those in age-matched individuals without cancer from the Legacy cohort^{28,29}, although conclusions for AZ are more limited by the very small sample size. While a relatively small number of patients with solid cancer had undetectable NAb against Delta (AZ, 36%; PZ, 8%), the proportion was higher overall than that in healthy controls. Our study is underpowered



to definitively ascertain whether cancer-specific factors impact the NAb response in patients with solid cancer or whether this is largely driven by age. While our data in this patient group are reassuring overall, it is important to acknowledge that NAb levels required to prevent infection may be higher than those needed for prevention of severe illness. Prevention of SARS-CoV-2 infection in patients with cancer, especially those in active treatment, is critical, as even asymptomatic infections can interrupt delivery of cancer care (that is, surgery, SACT or hospital appointments).

We observed only eight breakthrough SARS-CoV-2 infections (1% of vaccinated patients). However, the study period fell between February and May 2021 for most patients, representing a time of relatively low infection rates in the UK, at a time of declining Alpha VOC infections and before the current Delta surge. During a similar time period (December 2020–May 2021), a longitudinal community-surveillance study of the general UK population showed that vaccination with one dose of AZ or PZ reduced infections by 61–66% (further reduced by 79–80% with a second dose)⁵⁷. Our low rate of breakthrough infections in patients with cancer is reassuring, but, as CAPTURE was not designed to assess vaccine efficacy, this needs to be considered with caution. Further, the behavior of patients with cancer may have contributed to the results, as they are likely to exercise caution especially before full vaccination. An ongoing aim of the CAPTURE study includes collection of data on breakthrough infections.

The strengths of our study include a large, prospectively recruited cohort with comparison across humoral and cell-mediated immunity against VOC, which has so far been lacking in studies of patients with cancer. There are limitations in our dataset; first, while we performed an age-matched comparison with Legacy data, the analysis was limited to a small number of patients and would benefit from further validation. Second, we relied on opportunistic sampling given restrictions on nonessential travel and hospital attendance leading to missed sampling points, particularly in occasional hospital attendees. Finally, validation of findings in solid cancer type or treatment subgroups in larger datasets or through meta-analyses will be important especially for detection of marginal differences.

In conclusion, our results have clear implications for the management of patients with cancer. Our data support the prioritization of patients with cancer for booster vaccine doses, suggesting that the highest priority should be given to those with hematological malignancies, followed by patients with advanced age, especially if they were vaccinated with AZ. Personal risk mitigation and ongoing public health measures remain relevant for at-risk groups, especially when community transmission of VOC is high. Moving forward, defining the correlates of immune protection (including humoral and cellular responses) will be critical to guide decision making. Longitudinal evaluation will define the durability and nature of immune protection and the occurrence of breakthrough infection in the context of potentially waning antibody responses. As such, an adaptable framework within ongoing prospective efforts will be instrumental to safely navigate the next phase of the pandemic for our patients.

Methods

Study design. CAPTURE (NCT03226886) is a prospective, longitudinal cohort study that commenced recruitment in May 2020 and continues to enroll patients at the Royal Marsden NHS Foundation Trust. The study design has been previously published²⁶. In brief, adult patients with current or history of invasive cancer are eligible for enrollment. Inclusion criteria are intentionally broad, and patients are recruited irrespective of cancer type, stage or treatment. Patients recruited to the CAPTURE study who have received at least one dose of COVID-19 vaccine will be included in an analysis to explore vaccine immunogenicity in patients with cancer. Patients are included in the analysis regardless of prior SARS-CoV-2 infection status. The primary outcome for this analysis will be the seroconversion rate in patients with cancer at 14–28 d following the second dose of vaccine. At establishment of the study protocol, there was no prior published data of seroconversion in patients with cancer in this setting; and thus sample size was

exploratory. The most precise estimate of seroconversion in patients with cancer would therefore be achieved through recruitment of as many patients as possible in the time period.

CAPTURE was approved as a substudy of TRACERx Renal (NCT03226886). TRACERx Renal was initially approved by the NRES Committee London, Fulham, on 17 January 2012. The TRACERx Renal substudy CAPTURE was submitted as part of Substantial Amendment 9 and approved by the Health Research Authority on 30 April 2020 and the NRES Committee London, Fulham, on 1 May 2020. CAPTURE is being conducted in accordance with the ethical principles of the Declaration of Helsinki, Good Clinical Practice and applicable regulatory requirements. All patients provided written, informed consent to participate.

Study schedule and follow-up. Clinical data and sample collection for participating patients with cancer is performed at baseline (before the first dose of vaccine or within 14 d of the first dose of vaccine) and at time points FU1 (2–4 weeks after the first dose of vaccine), FU2 (within 14 d before the second vaccine) and FU3 (2–4 weeks after the second dose of vaccine) (Fig. 1a and the Nature Research Reporting Summary).

Patient data and sample sources. Demographic, epidemiological and clinical data (for example, cancer type, cancer stage, treatment history) were collected from the internal electronic patient record, and pseudonymized data were entered into a cloud-based electronic database (Ninox Software). Regarding SACT, we deemed chemotherapy, targeted therapy (small-molecule inhibitors or monoclonal antibodies) or endocrine therapy to be current if given within 28 d of vaccination. CPI given within 6 months was considered significant given prolonged receptor occupancy with these agents⁵⁸. Concomitant medications were recorded for corticosteroids (considered significant if an equivalent of >10 mg prednisolone was given for at least 7 d), G-CSF (when given within 48 h of vaccination or 5 d if it was a pegylated preparation) and other immunosuppressive drugs taken within 48 h of vaccination.

Patients were grouped by cancer diagnosis (solid versus hematological malignancy) for downstream analysis. When two independent diagnoses of cancer were identified in the same patient, the case was reviewed by two clinicians (S.T.C.S. and A.M.S.), and the highest stage and/or cancer receiving active treatment was used for classification. Solid cancers were subdivided by anatomical systems (Table 1), with 21 patients assigned to the 'solid other' category consisting of endocrine and neuroendocrine tumors, sarcoma and gastrointestinal stromal tumors and central nervous system tumors. Patients with hematological malignancies were grouped by conventional subtypes, although one patient with aplastic anemia (CV0611) could not be intuitively grouped with those with other hematological disorders and was excluded from subgroup analyses.

Detailed sampling schedule and methodology have been previously described²⁶. Study biospecimens included per-protocol blood samples, oropharyngeal swabs and cryostored serum from routine clinical investigations. Collected data and study samples are de-identified and stored with only the study-specific study identification number.

Comparison with healthy individuals. Healthy individuals were included from the previously published Legacy study for comparison^{28,29}. The Legacy study includes healthy individuals vaccinated with PZ or AZ. To account for the heterogeneity of both cohorts, we selected cases based on age, type of vaccine and infection status. We only included blood samples taken between 14 and 42 d after the second dose. Infection status was self-reported for the LEGACY study^{28,29}. For individuals vaccinated with PZ, we only considered infection-naïve individuals. Patients with cancer and healthy controls were grouped into two age groups for comparison (40–54 years and 55 years and over). Individuals vaccinated with AZ were compared to patients with cancer independent of previous infection, and only individuals between 40 and 59 years of age were selected for comparison. T cell responses were compared to those from a group of healthcare professionals recruited to the CAPTURE study ($n = 25$, Supplementary Table 8).

Definition of previous SARS-CoV-2 infection. Most patients underwent RT-PCR screening as part of routine clinical care. To account for asymptomatic infections and/or symptomatic infections not confirmed by RT-PCR, we considered patients to have had previous SARS-CoV-2 infection if they had either (1) a previous SARS-CoV-2 positive RT-PCR test result and/or (2) a positive anti-S1 IgG ELISA result before vaccination.

World Health Organization classification of COVID-19 severity. We classified COVID-19 severity according to the WHO clinical progression scale³¹: uninfected (uninfected, no viral RNA detected), 0; asymptomatic (viral RNA and/or S1-reactive IgG detected), 1; mild (ambulatory) (symptomatic, independent), 2; symptomatic (assistance needed), 3; moderate (hospitalized, no oxygen therapy) (if hospitalized for isolation only, status was record as for ambulatory patients), 4; oxygen given by mask or nasal prongs, 5; severe (hospitalized, oxygen given by non-invasive ventilation or high flow), 6; intubation and mechanical ventilation ($pO_2/FiO_2 \geq 150$ or $SpO_2/FiO_2 \geq 200$), 7; mechanical ventilation ($pO_2/FiO_2 < 150$ ($SpO_2/FiO_2 < 200$)) or vasopressors, 8; mechanical ventilation ($pO_2/FiO_2 < 150$) and vasopressors, dialysis or extracorporeal membrane oxygenation, 9; dead, 10.

Handling of whole-blood samples. All blood samples and isolated products were handled in a CL2 laboratory inside a biosafety cabinet using appropriate personal protective equipment and safety measures, which were in accordance with a risk assessment and a standard operating procedure approved by the safety, health and sustainability committee of the Francis Crick Institute. For indicated experiments, serum or plasma samples were inactivated by heating at 56 °C for 30 min before use, after which they were used in a CL1 laboratory.

Plasma and PBMC isolation. Whole blood was collected in EDTA tubes (VWR) and stored at 4 °C until processing. All samples were processed within 24 h. Time of blood draw, processing and freezing was recorded for each sample. Before processing, tubes were brought to room temperature (RT). PBMCs and plasma were isolated by density gradient centrifugation using prefilled centrifugation tubes (pluriSelect). Up to 30 ml undiluted blood was added on top of the sponge and centrifuged for 30 min at 1,000g and RT. Plasma was carefully removed and then centrifuged for 10 min at 4,000g to remove debris, aliquoted and stored at –80 °C. The cell layer was then collected and washed twice with PBS by centrifugation for 10 min at 300g and RT. PBMCs were resuspended in Recovery Cell Culture Freezing Medium (Fisher Scientific) containing 10% DMSO, placed overnight in CoolCell freezing containers (Corning) at –80 °C and then stored in liquid nitrogen.

Serum isolation. Whole blood was collected in serum coagulation tubes (Vacuette CAT tubes, Greiner) for serum isolation and stored at 4 °C until processing. All samples were processed within 24 h. Time of blood draw, processing and freezing was recorded for each sample. Tubes were centrifuged for 10 min at 2,000g and 4 °C. Serum was separated from the clotted portion, aliquoted and stored at –80 °C.

S1-reactive IgG ELISA. Ninety-six-well MaxiSorp plates (Thermo Fisher Scientific) were coated overnight at 4 °C with purified S1 protein in PBS (3 µg ml⁻¹ per well in 50 µl) and blocked for 1 h in blocking buffer (PBS, 5% milk, 0.05% Tween-20 and 0.01% sodium azide). Sera were diluted in blocking buffer (1:50). Serum (50 µl) was then added to wells and incubated for 2 h at RT. After washing four times with PBS-T (PBS, 0.05% Tween-20), plates were incubated with alkaline phosphatase-conjugated goat anti-human IgG antibody (1:1,000, Jackson ImmunoResearch) for 1 h. Plates were developed by adding 50 µl alkaline phosphatase substrate (Sigma-Aldrich) for 15–30 min after six washes with PBS-T. Optical densities were measured at 405 nm in a microplate reader (Tecan). CR3022 (Absolute Antibodies) was used as a positive control. The cutoff for a positive response was defined as the mean negative value multiplied by 0.35× the mean positive value.

Virus variants and culture. The SARS-CoV-2 reference isolate (referred to as ‘WT’) was hCoV19/England/02/2020, obtained from the Respiratory Virus Unit, Public Health England (GISAID EpiCov accession, EPI_ISL_407073). The B.1.1 strain (‘D614G’) was isolated from a swab from an infected healthcare worker at UCLH, obtained through the SAFER study and carries only the D614G substitution in its S protein. The B.1.1.7 isolate (‘B.1.1.7’) was hCoV19/England/204690005/2020, which carries D614G, Δ69–70, Δ144, N501Y, A570D, P681H, T716I, S982A and D1118H mutations, obtained from Public Health England through W. Barclay, Imperial College London through the Genotype-to-Phenotype National Virology Consortium. The B.1.351 viral isolate was 501Y.V2.HV001, which carries D614G, L18F, D80A, D215G, Δ242–244, K417N, E484K, N501Y, A701V mutations, and was kindly provided by A. Sigal and T. de Oliveira (University of KwaZulu-Natal, Durban, South Africa); sequencing of received viral isolates identified sequences corresponding to Q677H and R682W substitutions at the furin cleavage site in approximately 50% of the genomes, which was maintained upon passage in cell culture. The B.1.617.2 isolate was MS066352H (GISAID accession number EPI_ISL_1731019), which carries T19R, K77R, G142D, Δ156–157/R158G, A222V, L452R, T478K, D614G, P681R and D950N mutations, and was kindly provided by W. Barclay, Imperial College London through the Genotype-to-Phenotype National Virology Consortium. All viral isolates were propagated in Vero V1 cells. Briefly, 50% confluent monolayers of Vero E6 cells were infected with the given SARS-CoV-2 strains at an MOI of approximately 0.001. Cells were washed once with DMEM (Sigma, D6429), and then 5 ml virus inoculum prepared in DMEM was added to each T175 flask and incubated at RT for 30 min. DMEM with 1% FCS (Biosera, FB-1001/500) was added to each flask. Cells were incubated at 37 °C with 5% CO₂ for 4 d until extensive cytopathogenic effects were observed. Supernatant was collected and clarified by centrifugation at 2,000 r.p.m. for 10 min in a benchtop centrifuge. Supernatant was aliquoted and frozen at –80 °C.

Viral PCR and sequencing. All virus stocks generated for use in neutralization assays were validated by sequencing before use. To confirm the identity of cultured VOC samples, 8 µl viral RNA was prepared for sequencing by the ARTIC method (<https://www.protocols.io/view/ncov-2019-sequencingprotocol-v3-locost-bh42j8ye>) and sequenced on the ONT GridION platform to >30,000 reads per sample. Data were demultiplexed and processed using the viralrecon pipeline (<https://github.com/nf-core/viralrecon>).

High-throughput live virus-microneutralization assay. High-throughput live virus-microneutralization assays were performed as described previously⁵⁹. Briefly, Vero E6 cells (Institut Pasteur) or Vero E6 cells expressing ACE2 and TMPRSS2 (VAT-1) (Centre for Virus Research)⁶⁰ at 90–100% confluency in 384-well format were first titrated with varying MOI of each SARS-CoV-2 variant and varying concentrations of a control monoclonal nanobody to normalize for possible replicative differences between variants and select conditions equivalent to those observed with the WT virus. Following this calibration, cells were infected in the presence of serial dilutions of patient serum samples. After infection (24 h, Vero E6, Pasteur; 16 h, VAT-1), cells were fixed with a final concentration of 4% formaldehyde, permeabilized with 0.2% Triton X-100 and 3% BSA in PBS (vol/vol) and stained for the SARS-CoV-2 N protein using the Alexa 488-labeled CR3009 antibody produced in house and for cellular DNA using DAPI⁶¹. Whole-well imaging at 5× was carried out using an Opera Phenix system (PerkinElmer), and fluorescent areas and intensities were calculated using Phenix-associated software (Harmony 9, PerkinElmer). Inhibition was estimated from the measured area of infected cells divided by the total area occupied by all cells. The inhibitory profile of each serum sample was estimated by fitting a four-parameter dose–response curve executed in SciPy. NAbT are reported as the fold dilution of serum required to inhibit 50% of viral replication (IC₅₀) and are further annotated if they lie above the quantitative (complete inhibition) range or below the quantitative range but still within the qualitative range (that is, partial inhibition is observed, but a dose–response curve cannot be fit because it does not sufficiently span the IC₅₀) or if they show no inhibition at all. IC₅₀ values above the quantitative detection limit of the assay (>2,560) were recoded as 3,000; IC₅₀ values below the quantitative limit of the assay (<40) but within the qualitative range were recoded as 39, and data below the qualitative range (that is, no response observed) were recoded as 35.

Enzyme-linked immunospot assay. IFN-γ-precoated ELISpot (Mabtech) plates were blocked with complete medium (RPMI, 5% human AB serum) before 300,000 PBMCs were seeded per well and stimulated for 18 h. Synthetic SARS-CoV-2 PepTivator peptides (Miltenyi Biotec), consisting of 15-mer sequences with an overlap of 11 amino acids, were used at a final concentration of 1 µg ml⁻¹ per peptide as follows: (1) PepTivator SARS-CoV-2 Prot_S1 (amino acids 1–692), (2) PepTivator SARS-CoV-2 Prot_S (covering sequences 304–338, 421–475, 492–519, 683–707, 741–770, 785–802 and 885–1,273) and PepTivator SARS-CoV-2 Prot_S+ with amino acids 689–895 combined into a single pool broadly representing S2, (3) PepTivator SARS-CoV-2 Prot_M (covering the complete M glycoprotein), (4) PepTivator SARS-CoV-2 Prot_N (covering the complete N phosphoprotein), (5) PepTivator SARS-CoV-2 Prot_S B.1.1.7 Mutation Pool (34 peptides covering mutated regions in the S protein of the Alpha VOC), (6) PepTivator SARS-CoV-2 Prot_S B.1.617.2 Mutation Pool, which selectively covers mutated regions (32 peptides covering mutated regions in the S protein of the Delta VOC).

Plates were developed with human biotinylated IFN-γ-detection antibody (7-B6-1-ALP, 1:200), followed by incubation with BCIP/NBT Phosphatase Substrate (SeraCare). SFU were quantified with Mabtech ASTOR ELISpot plate reader. To quantify positive peptide-specific responses, values of spots in unstimulated wells were subtracted from those from peptide-stimulated wells, and the results were expressed as SFU per million. Samples for which positive controls were <10 SFU per 10⁶ spots per well were excluded, as were samples with negative control >50 SFU per million. The cutoff threshold for a positive result was the mean of the negative control well plus 2×s.d. (24 SFU per million)⁶². The magnitude of the response (that is, SFU per million) could not be compared between SARS-CoV-2 WT and VOC due to the reduced number of peptides in VOC pools.

Multiplex immune assay for cytokines and chemokines. The Milliplex Human Cytokine Panel A immunoassay (Merck) was used to measure 15 protein targets in cell culture supernatants on the Bio-Plex platform (Bio-Rad Laboratories) using Luminex xMAP technology. Measured analytes included IFN-γ, IL-10, IL-12 p40, IL-12 p70, IL-13, IL-17A, IL-18, IL-2, IL-22, IL-4, IL-5, IL-9, IP-10, MCP-1 and TNF. All assays were conducted according to the manufacturer’s recommendations.

Quantification and statistical analysis. Data analysis and statistical analysis were performed in R version 3.6.1 in RStudio version 1.2.1335. Gaussian distribution was tested by the Kolmogorov–Smirnov test. Wilcoxon–Mann–Whitney, Kruskal–Wallis, χ^2 and Fisher’s exact tests were performed to determine statistical significance. Bonferroni correction was applied for multiple-comparison testing. *P* values <0.05 were considered significant. All tests were performed in a two-sided manner. Statistical details for each experiment are provided in figure legends. The ggplot2 package in R was used for data visualization, and illustrative figures were created at <https://biorender.com/>. Data are usually plotted as single data points and violin or box plots on a logarithmic scale. For box plots, boxes represent upper and lower quartiles, the line represents the median, and whiskers represent IQR×1.5. Notches represent confidence intervals of the median. The point range in violin plots denotes the median and upper and lower quartiles. Spearman rank correlation coefficients were calculated between all parameter pairs. Multivariate binary logistic regression analysis was performed using the glm function with

the stats package in R. Ordinal logistic regression was performed using the `orm` function with the `rms` package in R.

Reporting Summary. Further information on research design is available in the Nature Research Reporting Summary linked to this article.

Data availability

All requests for raw and analyzed data and the CAPTURE study protocol will be reviewed by the CAPTURE Trial Management Team, Skin and Renal Clinical Trials Unit, the Royal Marsden NHS Foundation Trust (CAPTURE@rmh.nhs.uk) to determine whether the request is subject to confidentiality and data-protection obligations. Materials used in this study will be made available upon request. There are restrictions to availability based on limited quantities. Response to any request for data and/or materials will be given within a 28-d period. Data and materials that can be shared would then be released upon completion of a material-transfer agreement. Source data are provided with this paper.

Received: 18 August 2021; Accepted: 17 September 2021;
Published online: 27 October 2021

References

- Harvey, W. T. et al. SARS-CoV-2 variants, spike mutations and immune escape. *Nat. Rev. Microbiol.* **19**, 409–424 (2021).
- Public Health England. *Confirmed Cases of COVID-19 Variants Identified in UK* <https://www.gov.uk/government/news/confirmed-cases-of-covid-19-variants-identified-in-uk> (2021).
- Public Health England and Department of Health and Social Care. *COVID-19: Guidance on Protecting People Defined on Medical Grounds as Extremely Vulnerable* <https://www.gov.uk/government/publications/guidance-on-shielding-and-protecting-extremely-vulnerable-persons-from-covid-19/19-july-guidance-on-protecting-people-who-are-clinically-extremely-vulnerable-from-covid-19> (2021).
- Sheikh, A., McMenamin, J., Taylor, B. & Robertson, C. SARS-CoV-2 Delta VOC in Scotland: demographics, risk of hospital admission, and vaccine effectiveness. *Lancet* **397**, 2461–2462 (2021).
- Brosh-Nissimov, T. et al. BNT162b2 vaccine breakthrough: clinical characteristics of 152 fully-vaccinated hospitalized COVID-19 patients in Israel. *Clin. Microbiol. Infect.* <https://doi.org/10.1016/j.cmi.2021.06.036> (2021).
- Lopez Bernal, J. et al. Effectiveness of the Pfizer–BioNTech and Oxford–AstraZeneca vaccines on COVID-19 related symptoms, hospital admissions, and mortality in older adults in England: test negative case–control study. *BMJ* **373**, n1088 (2021).
- Sung, H. et al. Global cancer statistics 2020: GLOBOCAN estimates of incidence and mortality worldwide for 36 cancers in 185 countries. *CA Cancer J. Clin.* **71**, 209–249 (2021).
- Kuderer, N. M. et al. Clinical impact of COVID-19 on patients with cancer (CCC19): a cohort study. *Lancet* **395**, 1907–1918 (2020).
- Grivas, P. et al. Association of clinical factors and recent anticancer therapy with COVID-19 severity among patients with cancer: a report from the COVID-19 and Cancer Consortium. *Ann. Oncol.* **32**, 787–800 (2021).
- Lee, L. Y. W. et al. COVID-19 prevalence and mortality in patients with cancer and the effect of primary tumour subtype and patient demographics: a prospective cohort study. *Lancet Oncol.* **21**, 1309–1316 (2020).
- Garassino, M. C. et al. COVID-19 in patients with thoracic malignancies (TERAVOLT): first results of an international, registry-based, cohort study. *Lancet Oncol.* **21**, 914–922 (2020).
- Ribas, A. et al. Priority COVID-19 vaccination for patients with cancer while vaccine supply is limited. *Cancer Discov.* **11**, 233–236 (2020).
- Department of Health and Social Care. *Joint Committee on Vaccination and Immunisation: advice on priority groups for COVID-19 vaccination, 30 December 2020* <https://www.gov.uk/government/publications/priority-groups-for-coronavirus-covid-19-vaccination-advice-from-the-jcvi-30-december-2020/joint-committee-on-vaccination-and-immunisation-advice-on-priority-groups-for-covid-19-vaccination-30-december-2020> (2021).
- Thakkar, A. et al. Seroconversion rates following COVID-19 vaccination among patients with cancer. *Cancer Cell* **39**, 1081–1090 (2021).
- Monin, L. et al. Safety and immunogenicity of one versus two doses of the COVID-19 vaccine BNT162b2 for patients with cancer: interim analysis of a prospective observational study. *Lancet Oncol.* **22**, 765–778 (2021).
- Massarweh, A. et al. Evaluation of seropositivity following BNT162b2 messenger RNA vaccination for SARS-CoV-2 in patients undergoing treatment for cancer. *JAMA Oncol.* **7**, 1–8 (2021).
- Addeo, A. et al. Immunogenicity of SARS-CoV-2 messenger RNA vaccines in patients with cancer. *Cancer Cell* **39**, 1091–1098 (2021).
- Herishanu, Y. et al. Efficacy of the BNT162b2 mRNA COVID-19 vaccine in patients with chronic lymphocytic leukemia. *Blood* **137**, 3165–3173 (2021).
- Lim, S. H. et al. Antibody responses after SARS-CoV-2 vaccination in patients with lymphoma. *Lancet Haematol.* **8**, e542–e544 (2021).
- Roeker, L. E. et al. COVID-19 vaccine efficacy in patients with chronic lymphocytic leukemia. *Leukemia* **35**, 2703–2705 (2021).
- Maneikis, K. et al. Immunogenicity of the BNT162b2 COVID-19 mRNA vaccine and early clinical outcomes in patients with haematological malignancies in Lithuania: a national prospective cohort study. *Lancet Haematol.* **8**, e583–e592 (2021).
- Ghione, P. et al. Impaired humoral responses to COVID-19 vaccination in patients with lymphoma receiving B-cell directed therapies. *Blood* **138**, 811–814 (2021).
- Parry, H. et al. Antibody responses after first and second COVID-19 vaccination in patients with chronic lymphocytic leukaemia. *Blood Cancer J.* **11**, 136 (2021).
- Ehmsen, S. et al. Antibody and T cell immune responses following mRNA COVID-19 vaccination in patients with cancer. *Cancer Cell* **39**, 1034–1036 (2021).
- Grifoni, A. et al. Targets of T cell responses to SARS-CoV-2 coronavirus in humans with COVID-19 disease and unexposed individuals. *Cell* **181**, 1489–1501 (2020).
- Au, L. et al. Cancer, COVID-19, and antiviral immunity: the CAPTURE study. *Cell* **183**, 4–10 (2020).
- Bange, E. M. et al. CD8⁺ T cells contribute to survival in patients with COVID-19 and hematologic cancer. *Nat. Med.* **27**, 1280–1289 (2021).
- Wall, E. C. et al. AZD1222-induced neutralising antibody activity against SARS-CoV-2 Delta VOC. *Lancet* **398**, 207–209 (2021).
- Wall, E. C. et al. Neutralising antibody activity against SARS-CoV-2 VOCs B.1.617.2 and B.1.351 by BNT162b2 vaccination. *Lancet* **397**, 2331–2333 (2021).
- Carr, E. J. et al. Neutralising antibodies after COVID-19 vaccination in UK haemodialysis patients. *Lancet* **398**, 1038–1041 (2021).
- WHO Working Group on the Clinical Characterisation and Management of COVID-19 infection. A minimal common outcome measure set for COVID-19 clinical research. *Lancet Infect. Dis.* **20**, e192–e197 (2020).
- Thakkar, A. et al. Patterns of seroconversion for SARS-CoV-2 IgG in patients with malignant disease and association with anticancer therapy. *Nat. Cancer* **2**, 392–399 (2021).
- Greenberger, L. M. et al. Antibody response to SARS-CoV-2 vaccines in patients with hematologic malignancies. *Cancer Cell* **39**, 1031–1033 (2021).
- Shrotri, M. et al. Spike-antibody responses to ChAdOx1 and BNT162b2 vaccines by demographic and clinical factors (Virus Watch study). Preprint at <https://doi.org/10.1101/2021.05.12.21257102> (2021).
- Earle, K. A. et al. Evidence for antibody as a protective correlate for COVID-19 vaccines. *Vaccine* **39**, 4423–4428 (2021).
- Wang, Z. et al. mRNA vaccine-elicited antibodies to SARS-CoV-2 and circulating variants. *Nature* **592**, 616–622 (2021).
- Demonbreun, A. R. et al. Comparison of IgG and neutralizing antibody responses after one or two doses of COVID-19 mRNA vaccine in previously infected and uninfected individuals. *EclinicalMedicine* **38**, 101018 (2021).
- Khoury, D. S. et al. Neutralizing antibody levels are highly predictive of immune protection from symptomatic SARS-CoV-2 infection. *Nat. Med.* **27**, 1205–1211 (2021).
- Bergwerk, M. et al. COVID-19 breakthrough infections in vaccinated health care workers. *N. Engl. J. Med.* <https://doi.org/10.1056/NEJMoa2109072> (2021).
- Collier, D. A. et al. Age-related immune response heterogeneity to SARS-CoV-2 vaccine BNT162b2. *Nature* **596**, 417–422 (2021).
- Lopez Bernal, J. et al. Effectiveness of COVID-19 vaccines against the B.1.617.2 (Delta) variant. *N. Engl. J. Med.* **385**, 585–594 (2021).
- Voysey, M. et al. Single-dose administration and the influence of the timing of the booster dose on immunogenicity and efficacy of ChAdOx1 nCoV-19 (AZD1222) vaccine: a pooled analysis of four randomised trials. *Lancet* **397**, 881–891 (2021).
- Parry, H. et al. Extended interval BNT162b2 vaccination enhances peak antibody generation in older people. Preprint at <https://doi.org/10.1101/2021.05.15.21257017> (2021).
- Kamar, N. et al. Three doses of an mRNA COVID-19 vaccine in solid-organ transplant recipients. *N. Engl. J. Med.* **385**, 661–662 (2021).
- Hall, V. G. et al. Randomized trial of a third dose of mRNA-1273 vaccine in transplant recipients. *N. Engl. J. Med.* **385**, 1244–1246 (2021).
- Normark, J. et al. Heterologous ChAdOx1 nCoV-19 and mRNA-1273 vaccination. *N. Engl. J. Med.* **385**, 1049–1051 (2021).
- Barros-Martins, J. et al. Immune responses against SARS-CoV-2 variants after heterologous and homologous ChAdOx1 nCoV-19/BNT162b2 vaccination. *Nat. Med.* **27**, 1525–1529 (2021).
- Callaway, E. Mix-and-match COVID vaccines trigger potent immune response. *Nature* **593**, 491 (2021).
- Spencer, A. J. et al. Heterologous vaccination regimens with self-amplifying RNA and adenoviral COVID vaccines induce robust immune responses in mice. *Nat. Commun.* **12**, 2893 (2021).
- Hill, J. A., Ujjani, C. S., Greninger, A. L., Shadman, M. & Gopal, A. K. Immunogenicity of a heterologous COVID-19 vaccine after failed vaccination in a lymphoma patient. *Cancer Cell* **39**, 1037–1038 (2021).

51. Tarke, A. et al. Impact of SARS-CoV-2 variants on the total CD4⁺ and CD8⁺ T cell reactivity in infected or vaccinated individuals. *Cell Rep. Med.* **2**, 100355 (2021).
52. Israelov, B. et al. Adaptive immune determinants of viral clearance and protection in mouse models of SARS-CoV-2. *Sci. Immunol.* **6**, eab14509 (2021).
53. McMahan, K. et al. Correlates of protection against SARS-CoV-2 in rhesus macaques. *Nature* **590**, 630–634 (2021).
54. Apostolidis, S. A. et al. Cellular and humoral immune responses following SARS-CoV-2 mRNA vaccination in patients with multiple sclerosis on anti-CD20 therapy. *Nat. Med.* <https://doi.org/10.1038/s41591-021-01507-2> (2021).
55. Passaro, A. et al. Severity of COVID-19 in patients with lung cancer: evidence and challenges. *J. Immunother. Cancer* **9**, e002266 (2021).
56. de Joode, K. et al. Dutch Oncology COVID-19 Consortium: outcome of COVID-19 in patients with cancer in a nationwide cohort study. *Eur. J. Cancer* **141**, 171–184 (2020).
57. Pritchard, E. et al. Impact of vaccination on new SARS-CoV-2 infections in the United Kingdom. *Nat. Med.* **27**, 1370–1378 (2021).
58. Fessas, P., Lee, H., Ikemizu, S. & Janowitz, T. A molecular and preclinical comparison of the PD-1-targeted T-cell checkpoint inhibitors nivolumab and pembrolizumab. *Semin. Oncol.* **44**, 136–140 (2017).
59. Faulkner, N. et al. Reduced antibody cross-reactivity following infection with B.1.1.7 than with parental SARS-CoV-2 strains. *eLife* **10**, e69317 (2021).
60. Rihn, S. J. et al. A plasmid DNA-launched SARS-CoV-2 reverse genetics system and coronavirus toolkit for COVID-19 research. *PLoS Biol.* **19**, e3001091 (2021).
61. van den Brink, E. N. et al. Molecular and biological characterization of human monoclonal antibodies binding to the spike and nucleocapsid proteins of severe acute respiratory syndrome coronavirus. *J. Virol.* **79**, 1635–1644 (2005).
62. Adriana, T. et al. Divergent trajectories of antiviral memory after SARS-CoV-2 infection. Preprint at <https://doi.org/10.21203/rs.3.rs-612205/v1> (2021).

Acknowledgements

We thank the CAPTURE trial team, including E. Carlyle, K. Edmonds and L. Del Rosario, as well as H. Ahmad, L. Holt, M. O'Flaherty, D. Kelly, R. Dhaliwal, N. Ash, M. Mumin, L. Dowdie, K. Kelly, F. Williams, T. Foley, C. Lewis, M. Ndlovu, S. Ali, K. Lingard, S. Sarker, M. Mangwende, N. Hunter, J. Korteweg, A. Murra and K. Peat. We thank the administrative team that delivered the RMH vaccine program, including E. Mossman and J. Codet-Boise. We thank clinical research network nurses for their input with consent and specimen collection including H. Evans, N. Evans, S. Cooper, S. Jain, S. White, L. Roland, L. Hobbs and J. Dobbyn. We acknowledge the tremendous support from clinical and research teams at participating units at the Royal Marsden Hospital, including E. Black, A. Dela Rosa, C. Pearce, J. Bazin, L. Conneely, C. Burrows, T. Brown, J. Tai, E. Lidington, H. Hogan, A. Upadhyay, D. Capdeferro, I. Potyka, A. Drescher, F. Baksh, M. Balcorta, C. Da Costa Mendes, J. Amorim, V. Orejudos and L. Davison. We also thank volunteer staff at the Francis Crick Institute, the Crick COVID-19 Consortium and A. Lilley for help with neutralizing assays. We thank B. Asare and E. Carr for their input. Due to the pace at which the field is evolving, we acknowledge researchers of COVID-19, particularly those furthering our understanding of the COVID-19 vaccine-induced immune response, and we apologize for work that was not cited. This research was funded in part by the National Institute for Health Research (NIHR) Biomedical Research Centre at the Royal Marsden NHS Foundation Trust (RMCC32), Cancer Research UK (CRUK) (grant reference number C50947/A18176). This work was supported by the Francis Crick Institute, which receives its core funding from CRUK (FC001988, FC001218, FC001099, FC001002, FC001078, FC001169, FC001030, FC0011104), the UK Medical Research Council (FC001988, FC001218, FC001099, FC001002, FC001078, FC001169, FC001030, FC0011104) and the Wellcome Trust (FC001988, FC001218, FC001099, FC001002, FC001078, FC001169, FC001030, FC0011104). For the purpose of open access, the authors have applied a CC BY public copyright licence to any author accepted manuscript version arising from this submission. TRACERx Renal is partly funded by the NIHR Biomedical Research Centre at the Royal Marsden Hospital and the ICR (A109). The CAPTURE study is sponsored by the Royal Marsden NHS Foundation Trust and funded from a grant from the Royal Marsden Cancer Charity. A. Rogiers is supported by an ESMO clinical research fellowship. R.J.W. and K.A.W. receive support from Rosetrees (M926). A.F. has received funding from the European Union's Horizon 2020 research and innovation program under Marie Skłodowska-Curie grant agreement no. 892360. S.T.C.S. is supported and funded by a CRUK Clinician PhD Fellowship award. L.A. is funded by the Royal Marsden Cancer Charity. F.B. is funded by Rosetrees Charity (grant reference M829). S.T. is funded by CRUK (grant reference number C50947/A18176), the NIHR Biomedical Research Centre at the Royal Marsden Hospital and the Institute of Cancer Research (grant reference number A109), the Kidney and Melanoma Cancer Fund of the Royal Marsden Cancer Charity, the Rosetrees Trust (grant reference number A2204), Ventana Medical Systems (grant reference numbers 10467 and 10530), the National Institutes of Health (US) and the Melanoma Research Alliance. A.M.S. received an educational grant from Janssen-Cilag. C. Swanton is funded by CRUK (TRACERx, PEACE and

CRUK Cancer Immunotherapy Catalyst Network), the CRUK Lung Cancer Centre of Excellence (C11496/A30025), the Rosetrees Trust, Butterfield and Stoneygate Trusts, the Novo Nordisk Foundation (ID16584), a Royal Society Professorship Enhancement award (RP/EA/180007), the NIHR Biomedical Research Centre at University College London Hospitals, the CRUK University College London Centre, the Experimental Cancer Medicine Centre and the Breast Cancer Research Foundation (BCRF 20-157). This work was supported by a Stand Up To Cancer-LUNGevity-American Lung Association Lung Cancer Interception Dream Team Translational research grant (grant number SU2C-AACR-DT23-17 to S.M. Dubinett and A.E. Spira). Stand Up To Cancer is a division of the Entertainment Industry Foundation. Research grants are administered by the American Association for Cancer Research, the scientific partner of SU2C. C. Swanton received an ERC Advanced Grant (PROTEUS) from the European Research Council under the European Union's Horizon 2020 research and innovation program (grant agreement no. 835297). C. Swanton is a Royal Society Napier Research Professor (RP150154). R.J.W. has received funding from the Francis Crick Institute, which receives its core funding by Wellcome (FC0010218), UKRI (FC0010218) and CRUK (FC0010218) and research funding from Wellcome (203135 and 222754), Rosetrees (M926) and the South African MRC.

Author contributions

Conceptualization, S.T., L.A. and S.T.C.S.; methodology, S.T., A.F., S.T.C.S., F.B., K.A.W., G. Kassiotis, M.W. and R.H. Software, M.G.; formal analysis, A.F., S.T.C.S., L.A., G.Kelly, K.A.W., R.J.W., R.H., M.W. and M.C.; investigation, A.F., S.T.C.S., L.A., F.B., B.S., C.L.G., W.X., K.A.W., M.C., A.A.-D., M.W. and R.H.; resources, S.T., A.F., L.A., L.A.B., F.B., S.T.C.S., B.S., C.L.G., B.W., W.X., M.C., C.G., R.L.S., C.L.G., M.G., F.G., O.C., Z.T. and I.L.; writing (review and editing), S.T., A.F., S.T.C.S., L.A., K.A.W., M.W., F.B., M.C., A.M.S., N.J.-H., B.S., Z.T., K.R., L.A.B., R.H., E.C., K.E., L.D.R., S.S., K.L., M.M., L.H., H.A., J.K., T.F., J.B., W.G., T.B., A.E.-H., W.X., C.L.G., D.D., E.C.W., A.A.-D., S.N., S.C., M.G., J.I.M., G. Kelly, K.P., D.K., A.M., K.K., M.O'F., L.D., N.A., F.G., R.L.S., G.G., D.M., F.K., W.C., J.P., S.R., J.M., O.C., C. Stephenson, A. Robinson, B.O., S.F., I.L., A. Rogiers, S.I., M.E., C.M., D.O., I.C., N.S., N.T., L.W., N.v.A., R.L.J. J.D., S. Banerjee, K.C.T., M.O'B., K.H., S. Bhide, A.O., A. Reid, K.Y., A.J.S.F., L.P., C. Swanton, S. Gandhi, S. Gamblin, L.D.V.B., G. Kassiotis, S.K., N.Y., S.J., E.N., M.H., S.W. and R.J.W.; data curation, S.T.C.S., A.M.S., N.J.-H., B.S., C.L.G., Z.T., S.R., J.M., O.C., C. Stephenson, A. Rogiers, B.O., I.L., A. Reid, A.F. and L.A.; writing (original draft), S.T., K.R., A.F., L.A. and S.T.C.S.; visualization, A.F., S.T.C.S., S.T. and L.A.; supervision, S.T.; trial conduct, S.T., S.T.C.S., L.A., E.C., L.D.R., K.E., J.L., N.Y., A. Rogiers, E.N. and S.K. All authors approved the final version of the manuscript.

Competing interests

S.T. has received speaking fees from Roche, AstraZeneca, Novartis and Ipsen. S.T. has filed the following patents: 'Indel mutations as a therapeutic target and predictive biomarker' (PCT/GB2018/051892 and PCT/GB2018/051893) and 'Clear Cell Renal Cell Carcinoma Biomarkers' (P113326GB). N.Y. has received conference support from Celgene. A. Rogiers received a speaker fee from Merck Sharp & Dohme. J.L. received research funding from Bristol Myers Squibb, Merck, Novartis, Pfizer, Achilles Therapeutics, Roche, Nektar Therapeutics, Covance, Immunocore, Pharmacyclics and Aveo and served as a consultant to Achilles, AstraZeneca, Boston Biomedical, Bristol Myers Squibb, Eisai, EUSA Pharma, GlaxoSmithKline, Ipsen, Imugene, Incyte, iOnctura, Kymab, Merck Serono, Nektar, Novartis, Pierre Fabre, Pfizer, Roche Genentech, Secarna and Vitaccess. I.C. has served as a consultant to Eli Lilly, Bristol Myers Squibb, MSD, Bayer, Roche, Merck Serono, Five Prime Therapeutics, AstraZeneca, OncXerna, Pierre Fabre, Boehringer Ingelheim, Incyte, Astellas, GSK, Sotio and Eisai and has received research funding from Eli Lilly and Janssen-Cilag. He has received honoraria from Eli Lilly, Eisai and Servier. A.O. acknowledges receipt of research funding from Pfizer and Roche; speaker fees from Pfizer, Seagen, Lilly and AstraZeneca; is an advisory board member of Roche, Seagen and AstraZeneca; has received conference support from Leo Pharmaceuticals, AstraZeneca–Daiichi Sankyo and Lilly. C. Swanton acknowledges grant support from Pfizer, AstraZeneca, Bristol Myers Squibb, Roche–Ventana, Boehringer Ingelheim, ArcherDx (collaboration in minimal residual disease sequencing technologies) and Ono Pharmaceutical; is an AstraZeneca advisory board member and the chief investigator for the MermaiD1 clinical trial; has consulted for Amgen, Pfizer, Novartis, GlaxoSmithKline, MSD, Bristol Myers Squibb, Celgene, AstraZeneca, Illumina, Genentech, Roche–Ventana, GRAIL, Medixi, Metabomed, Bicycle Therapeutics and the Sarah Cannon Research Institute; has stock options in ApoGen Biotechnologies, Epic Bioscience and GRAIL; and has stock options in and is a cofounder of Achilles Therapeutics. C. Swanton holds European patents relating to assay technology to detect tumor recurrence (PCT/GB2017/053289), target neoantigens (PCT/EP2016/059401), identify patient response to immune-checkpoint blockade (PCT/EP2016/071471), determine HLA LOH (PCT/GB2018/052004), predict survival rates of patients with cancer (PCT/GB2020/050221) and identify patients who respond to cancer treatment (PCT/GB2018/051912); a US patent related to detecting tumor mutations (PCT/US2017/28013); and both a European and US patent related to identifying insertion and deletion mutation targets (PCT/GB2018/051892). L.P. has received research funding from Pierre Fabre and honoraria from Pfizer, Ipsen, Bristol Myers Squibb and EUSA Pharma. S. Banerjee has received institutional research funding from AstraZeneca, Tesaro and GSK; speaker fees from Amgen, Pfizer, AstraZeneca, Tesaro, GSK, Clovis, Takeda, Immunogen and Mersana; and has an advisor role for Amgen, AstraZeneca,

Epsilogen, Genmab, ImmunoGen, Mersana, MSD, Merck Serono, OncXerna, Pfizer and Roche. W.C. has received honoraria from Janssen and AstraZeneca. A.F., S.T.C.S., L.A., K.A.W., M.W., F.B., M.C., A.M.S., N.J.-H., B.S., Z.T., K.R., L.A.B., R.H., E.C., K.E., L.D.R., S.S., K.L., M.M., L.H., H.A., J.K., T.F., J.B., W.G., T.B., A.E.-H., W.X., C.L.G., D.D., E.C.W., A.A.-D., S.N., S.C., M.G., J.L.M., G. Kelly, K.P., D.K., A.M., K.K., M.O'F., L.D., N.A., F.G., R.L.S., G.G., D.M., F.K., W.C., J.P., S.R., J.M., O.C., C. Stephenson, B.O., S.F., I.L., A. Reid, S.I., M.E., C.M., D.C., N.S., N.T., L.W., N.v.A., R.L.J., J.D., K.C.T., M.O'B., K.H., S. Bhide, K.Y., A.J.S.F., S. Gamblin, D.L.V.B., G. Kassiotis, S.K., N.Y., S.J., E.N., M.H., S.W. and R.J.W. have no conflicts of interest to declare.

Peer review information *Nature Cancer* thanks Ailong Huang and the other, anonymous, reviewer(s) for their contribution to the peer review of this work.

Reprints and permissions information is available at www.nature.com/reprints.

Publisher's note Springer Nature remains neutral with regard to jurisdictional claims in published maps and institutional affiliations.



Open Access This article is licensed under a Creative Commons Attribution 4.0 International License, which permits use, sharing, adaptation, distribution and reproduction in any medium or format, as long as you give appropriate credit to the original author(s) and the source, provide a link to the Creative Commons license, and indicate if changes were made. The images or other third party material in this article are included in the article's Creative Commons license, unless indicated otherwise in a credit line to the material. If material is not included in the article's Creative Commons license and your intended use is not permitted by statutory regulation or exceeds the permitted use, you will need to obtain permission directly from the copyright holder. To view a copy of this license, visit <http://creativecommons.org/licenses/by/4.0/>.

© The Author(s) 2021

Additional information

Extended data is available for this paper at <https://doi.org/10.1038/s43018-021-00274-w>.

Supplementary information The online version contains supplementary material available at <https://doi.org/10.1038/s43018-021-00274-w>.

Correspondence and requests for materials should be addressed to Samra Turajlic.

¹Cancer Dynamics Laboratory, the Francis Crick Institute, London, UK. ²Skin and Renal Units, the Royal Marsden NHS Foundation Trust, London, UK. ³Tuberculosis Laboratory, the Francis Crick Institute, London, UK. ⁴Wellcome Center for Infectious Disease Research in Africa, University of Cape Town, Observatory, Cape Town, Republic of South Africa. ⁵High Throughput Screening Laboratory, the Francis Crick Institute, London, UK. ⁶Department of Infectious Disease, Imperial College London, London, UK. ⁷Worldwide Influenza Centre, the Francis Crick Institute, London, UK. ⁸Haemato-oncology Unit, the Royal Marsden NHS Foundation Trust, London, UK. ⁹University College London Hospitals NHS Foundation Trust Biomedical Research Centre, London, UK. ¹⁰Structural Biology of Disease Processes Laboratory, the Francis Crick Institute, London, UK. ¹¹Flow Cytometry Scientific Technology Platform, the Francis Crick Institute, London, UK. ¹²Safety, Health & Sustainability, the Francis Crick Institute, London, UK. ¹³Scientific Computing Scientific Technology Platform, the Francis Crick Institute, London, UK. ¹⁴Metabolomics Scientific Technology Platform, the Francis Crick Institute, London, UK. ¹⁵Department of Bioinformatics and Biostatistics, the Francis Crick Institute, London, UK. ¹⁶Department of Pathology, the Royal Marsden NHS Foundation Trust, London, UK. ¹⁷Translational Cancer Biochemistry Laboratory, the Institute of Cancer Research, London, UK. ¹⁸Clinical Trials Unit, the Royal Marsden NHS Foundation Trust, London, UK. ¹⁹Lung Unit, the Royal Marsden NHS Foundation Trust, London, UK. ²⁰Breast Unit, the Royal Marsden NHS Foundation Trust, London, UK. ²¹Gastrointestinal Unit, the Royal Marsden NHS Foundation Trust, London, UK. ²²Department of Radiology, the Royal Marsden NHS Foundation Trust, London, UK. ²³Neuro-oncology Unit, the Royal Marsden NHS Foundation Trust, London, UK. ²⁴Clinical Oncology Unit, the Royal Marsden NHS Foundation Trust, London, UK. ²⁵Sarcoma Unit, the Royal Marsden NHS Foundation Trust and Institute of Cancer Research, London, UK. ²⁶Palliative Medicine, the Royal Marsden NHS Foundation Trust, London, UK. ²⁷Gynaecology Unit, the Royal Marsden NHS Foundation Trust, London, UK. ²⁸Anaesthetics, Perioperative Medicine and Pain Department, the Royal Marsden NHS Foundation Trust, London, UK. ²⁹Head and Neck Unit, the Royal Marsden NHS Foundation Trust, London, UK. ³⁰Targeted Therapy Team, The Institute of Cancer Research, London, UK. ³¹Acute Oncology Service, the Royal Marsden NHS Foundation Trust, London, UK. ³²Uro-oncology Unit, the Royal Marsden NHS Foundation Trust, Surrey, UK. ³³Cancer Evolution and Genome Instability Laboratory, the Francis Crick Institute, London, UK. ³⁴University College London Cancer Institute, London, UK. ³⁵Neurodegeneration Biology Laboratory, the Francis Crick Institute, London, UK. ³⁶UCL Queen Square Institute of Neurology, London, UK. ³⁷RNA Virus Replication Laboratory, the Francis Crick Institute, London, UK. ³⁸Retroviral Immunology Laboratory, the Francis Crick Institute, London, UK. ³⁹These authors contributed equally: Annika Fendler, Scott T.C. Shepherd, Lewis Au, Katalin A. Wilkinson, Mary Wu. *Lists of authors appears at the end of the paper. [✉]e-mail: samra.turajlic@crick.ac.uk

The Crick COVID-19 Consortium

Mary Wu^{5,39}, Ruth Harvey⁷, Simon Caidan¹², James I. MacRae¹⁴, Gavin Kelly¹⁵, Charles Swanton^{33,34}, Sonia Gandhi^{35,36}, Steve Gamblin¹⁰, David L. V. Bauer³⁷, George Kassiotis³⁸ and Michael Howell⁵

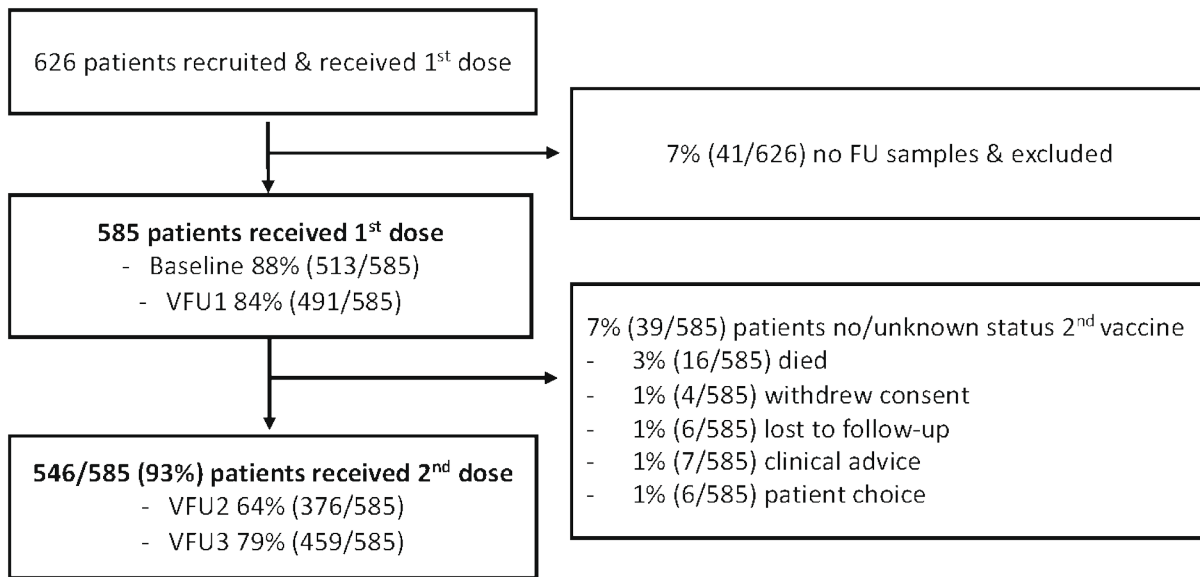
A full list of members appears in the Supplementary Information.

The CAPTURE Consortium

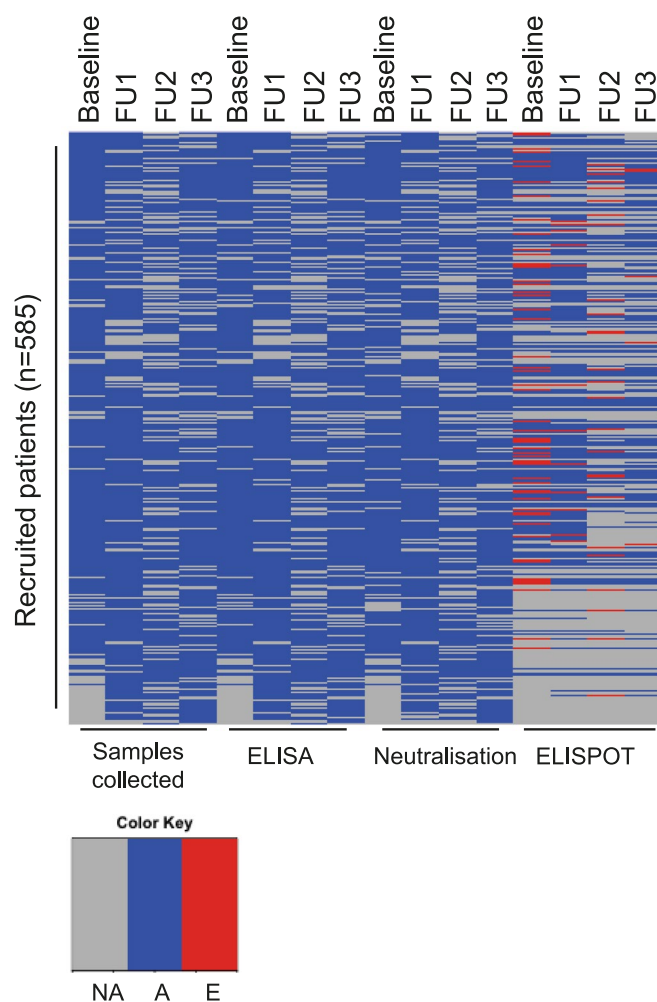
Annika Fendler^{1,39}, Scott T. C. Shepherd^{1,2,39}, Lewis Au^{1,2,39}, Katalin A. Wilkinson^{3,4,39}, Mary Wu^{5,39}, Fiona Byrne¹, Andreas M. Schmitt², Benjamin Shum^{1,2}, Laura Amanda Boos², Camille L. Gerard¹, Firza Gronthoud¹⁶, Christina Messiou²², David Cunningham²¹, Ian Chau²¹, Naureen Starling²¹, Nicholas Turner²⁰, Liam Welsh²³, Robin L. Jones²⁵, Joanne Droney²⁶, Susana Banerjee²⁷, Kate C. Tatham²⁸, Kevin Harrington^{29,30}, Shreerang Bhide^{29,30}, Alicia Okines^{20,31}, Alison Reid³², Kate Young², Andrew J. S. Furness², Lisa Pickering², George Kassiotis³⁸, Sacheen Kumar²¹, Nadia Yousaf^{19,31}, Shaman Jhanji²⁸, Emma Nicholson⁸, Robert J. Wilkinson^{3,4,6}, James Larkin² and Samra Turajlic^{1,2}

A full list of members appears in the Supplementary Information.

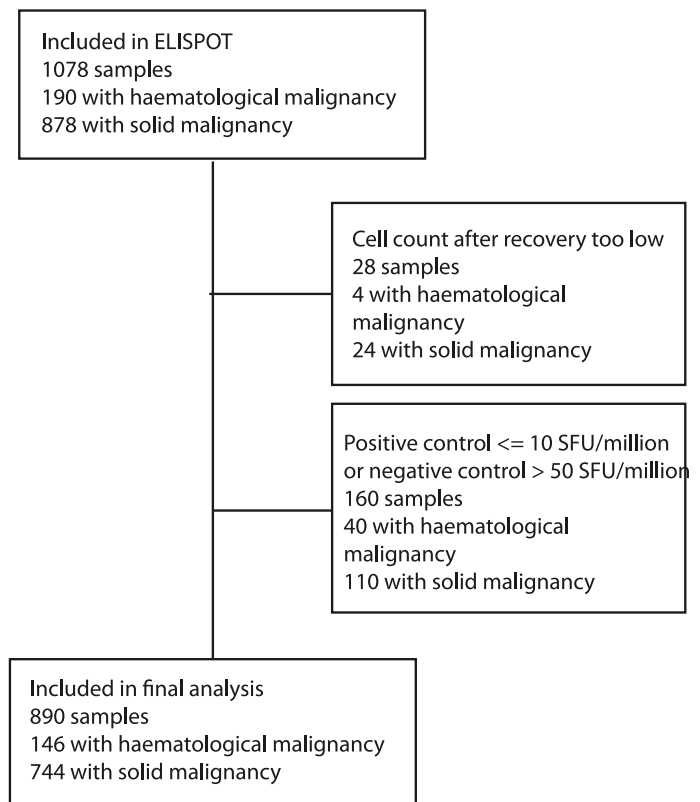
a



b

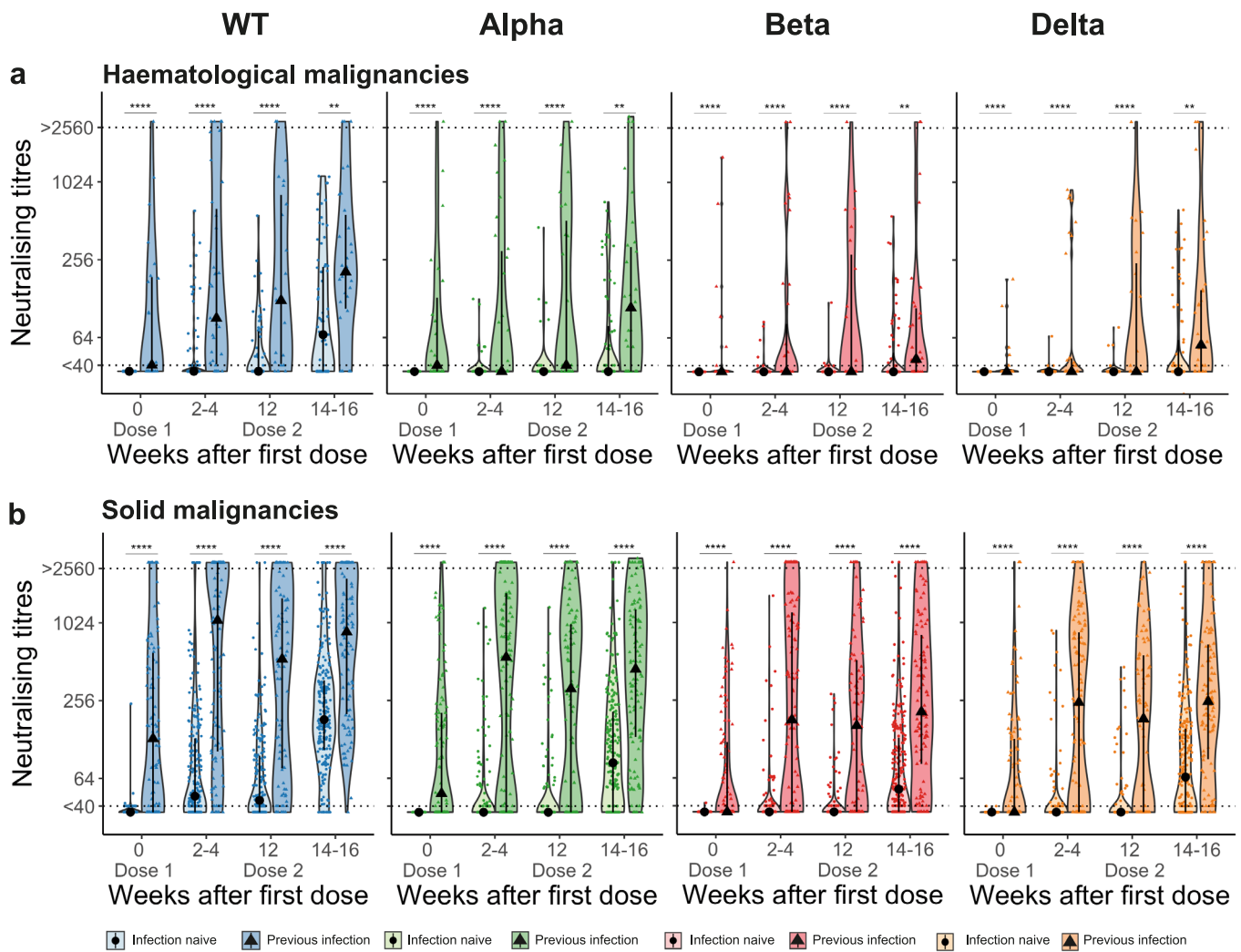


c

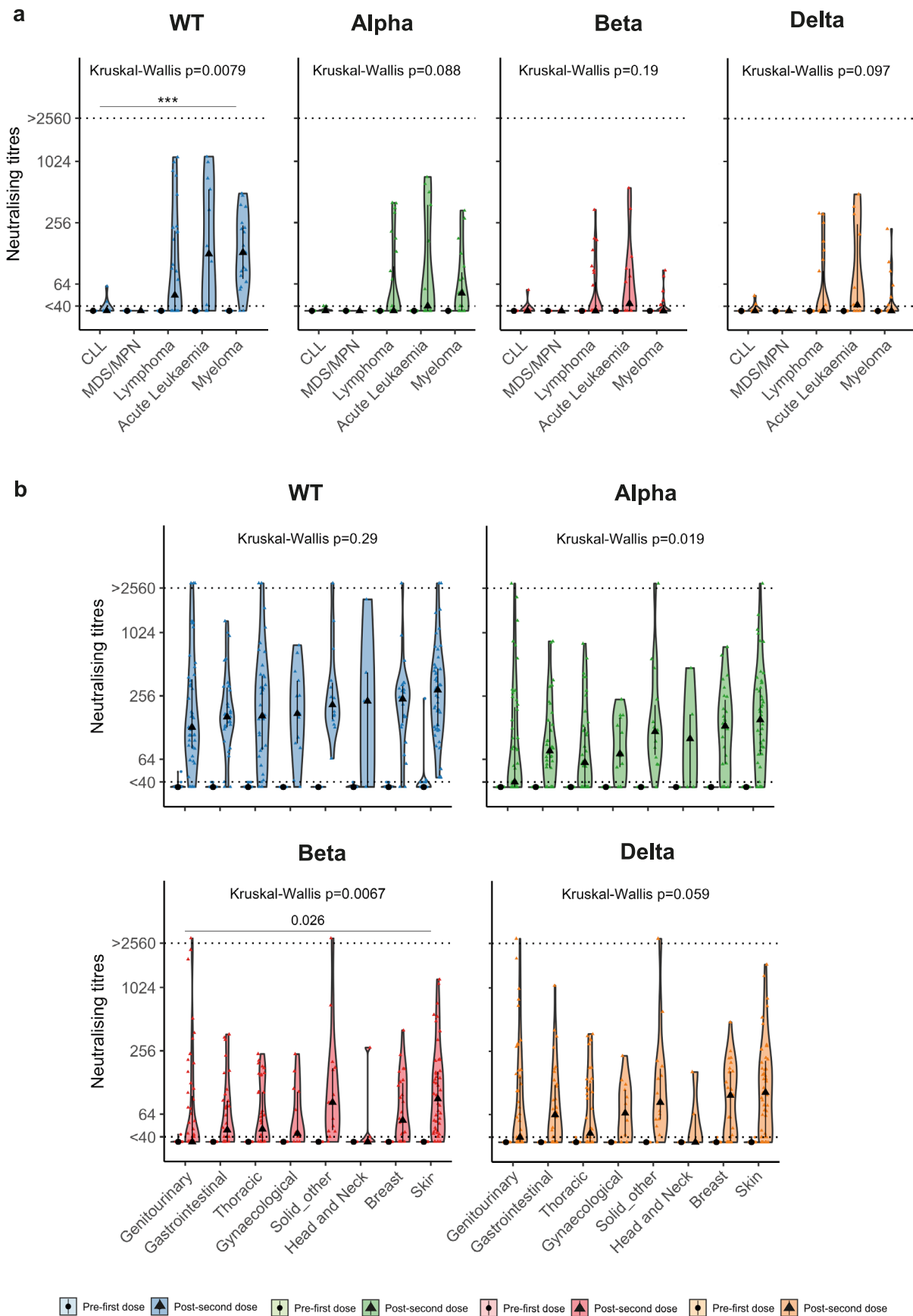


Extended Data Fig. 1 | See next page for caption.

Extended Data Fig. 1 | Overview of collected and analysed samples per patient. **a)** Consort diagram detailing the flow of patients into the CAPTURE Study and number of samples collected for each timepoint up to data lock on 15/06/2021. Baseline, prior to first vaccine dose or within 14 days of vaccination; FU1, follow-up 1: 2-4 weeks post-first vaccine dose; FU2, follow-up 2: within 14 days prior to second vaccination; FU3, follow-up 3: 2-4 weeks post-second vaccine dose. **b)** Blue rectangles indicate that a samples were collected or analysed (A), grey rectangles indicate that samples were not collected or analysed (NA), red rectangles indicate that samples were excluded from ELISPOT analysis either because cell numbers were too low, or positive/negative control failed in ELISPOT assay. **c)** Sampling and analysis schema for ELISPOT analysis. PBMC, peripheral blood mononuclear cells. NA, Not available, A, Analysed/Received, E, excluded.

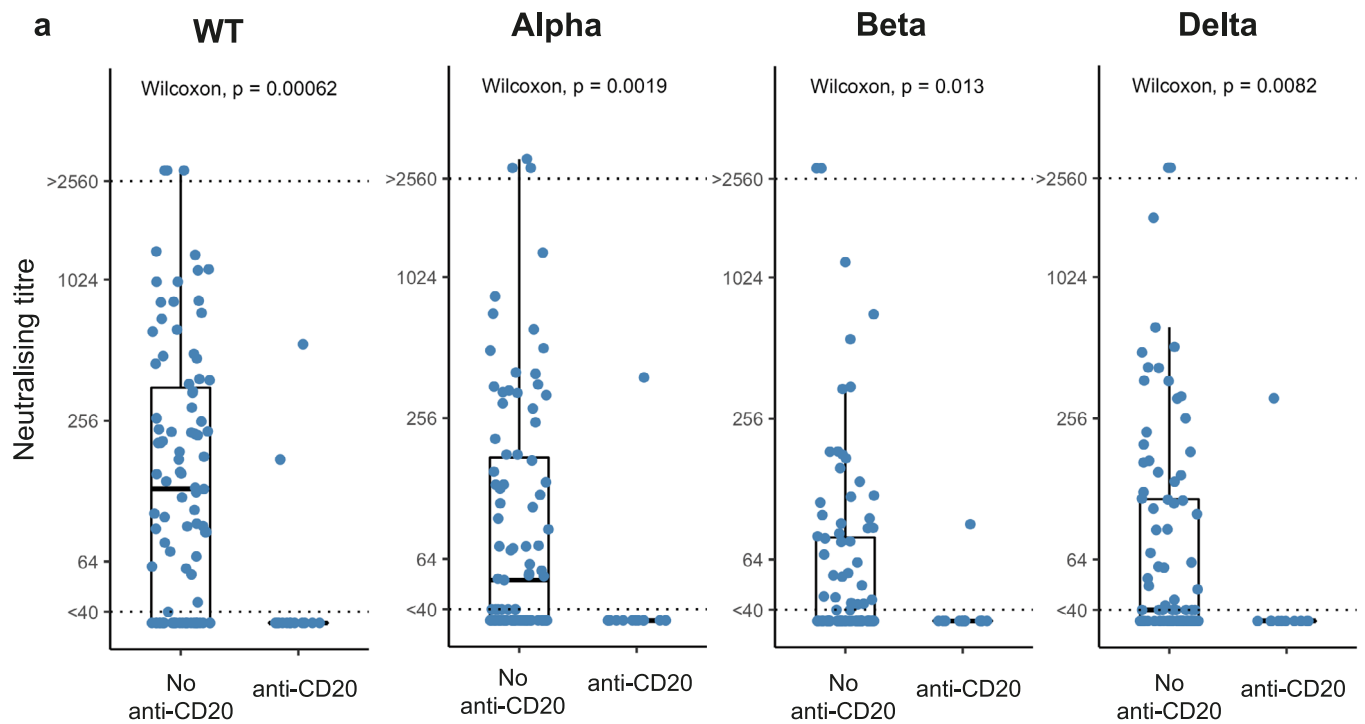


Extended Data Fig. 2 | Previous infection in patients with haematological and solid cancers. a) Comparison of NAbT against WT SARS-CoV-2, Alpha, Beta, and Delta VOCs in infection naïve ($n = 56/84/64/75$ patients at BL/FU1/FU2/FU3) vs previously SARS-CoV-2 infected ($n = 23/35/23/30$ patients at BL/FU1/FU2/FU3) patients with haematological malignancies, and **b)** in infection naïve ($n = 262/232/189/231$ patients at BL/FU1/FU2/FU3) vs previously SARS-CoV-2 infected ($n = 110/128/92/114$ patients at BL/FU1/FU2/FU3) patients with solid cancers Dotted line at <40 denotes the lower limit of detection, dotted line at >2560 denoted the upper limit of detection. Violin plots denote density of data points. PointRange denotes the median and the 25 and 75 percentiles. Dots represent individual samples. Significance was tested by two-sided Wilcoxon Mann-Whitney U test, $p < 0.05$ was considered significant. ns, non-significant * $p < 0.05$, ** $p < 0.01$, *** $p < 0.001$. AZ, AstraZeneca; NAbT, neutralising antibody titres; PZ, Pfizer; VOC, variant of concern. NA, not tested. BL, baseline; FU1, 21-56 days post first-vaccine; FU2, 14-28 days prior to second vaccine; FU3, 14-28days post second vaccine.

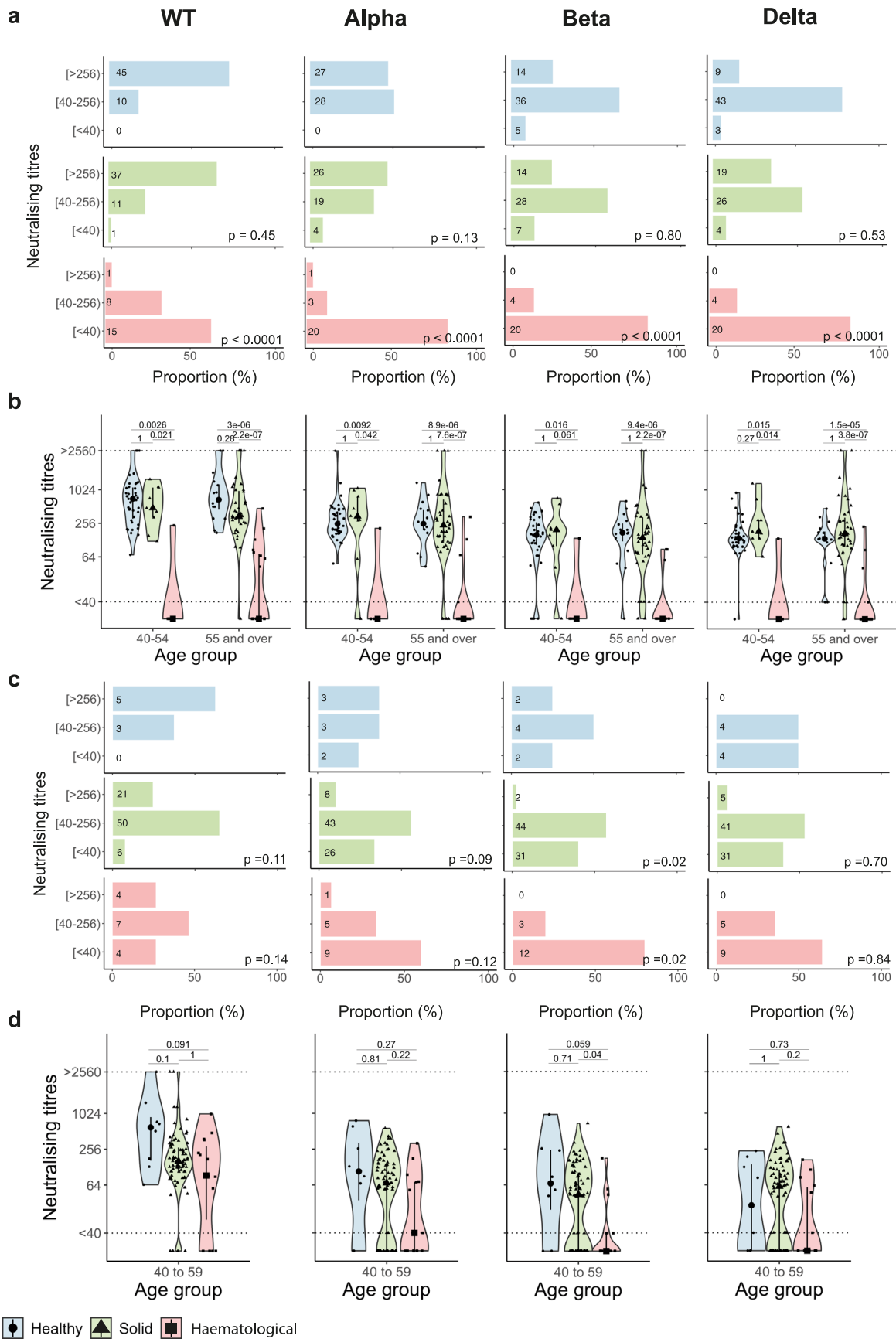


Extended Data Fig. 3 | See next page for caption.

Extended Data Fig. 3 | NAbT against WT SARS-CoV-2 and VOCs in haematological and solid cancer types. a) Comparison of NAbT WT SARS-CoV-2 and the three VOCs by cancer type in infection-naive patients with haematological malignancies (At BL/FU3: CLL: 3/11, MDS/MPN:5/4, Lymphoma: 23/28, Acute Leukaemia:16/13, Myeloma:8/19, 1 patient with aplastic anaemia not included in analysis) and **b)** solid tumours (At BL/FU3: Genitourinary: 56/51, GI: 35/34, Thoracic: 49/38, Gynae: 16/13, Solid_other: 13/14, H&N: 8/5, Breast: 26/26, Skin: 59/51). Dotted line at <40 denotes the lower limit of detection, dotted line at >2560 denoted the upper limit of detection. Violin plots denote density of data points. Pointrange denotes the median and the 25 and 75 percentiles. Dots represent individual samples. Significance post-second dose was tested by Kruskal Wallis test, $p < 0.05$ was considered significant, post-hoc test: two-sided Wilcoxon Mann-Whitney U test with Bonferroni correction was used for pairwise comparisons. Only comparisons with an adjusted p-value < 0.05 are denoted in the graph. * $p < 0.05$, ** $p < 0.01$, *** $p < 0.001$. GI, Gastrointestinal; Gynae, Gynaecological; H&N, Head & Neck; BL, baseline; FU3, 14-28days post second-vaccine.

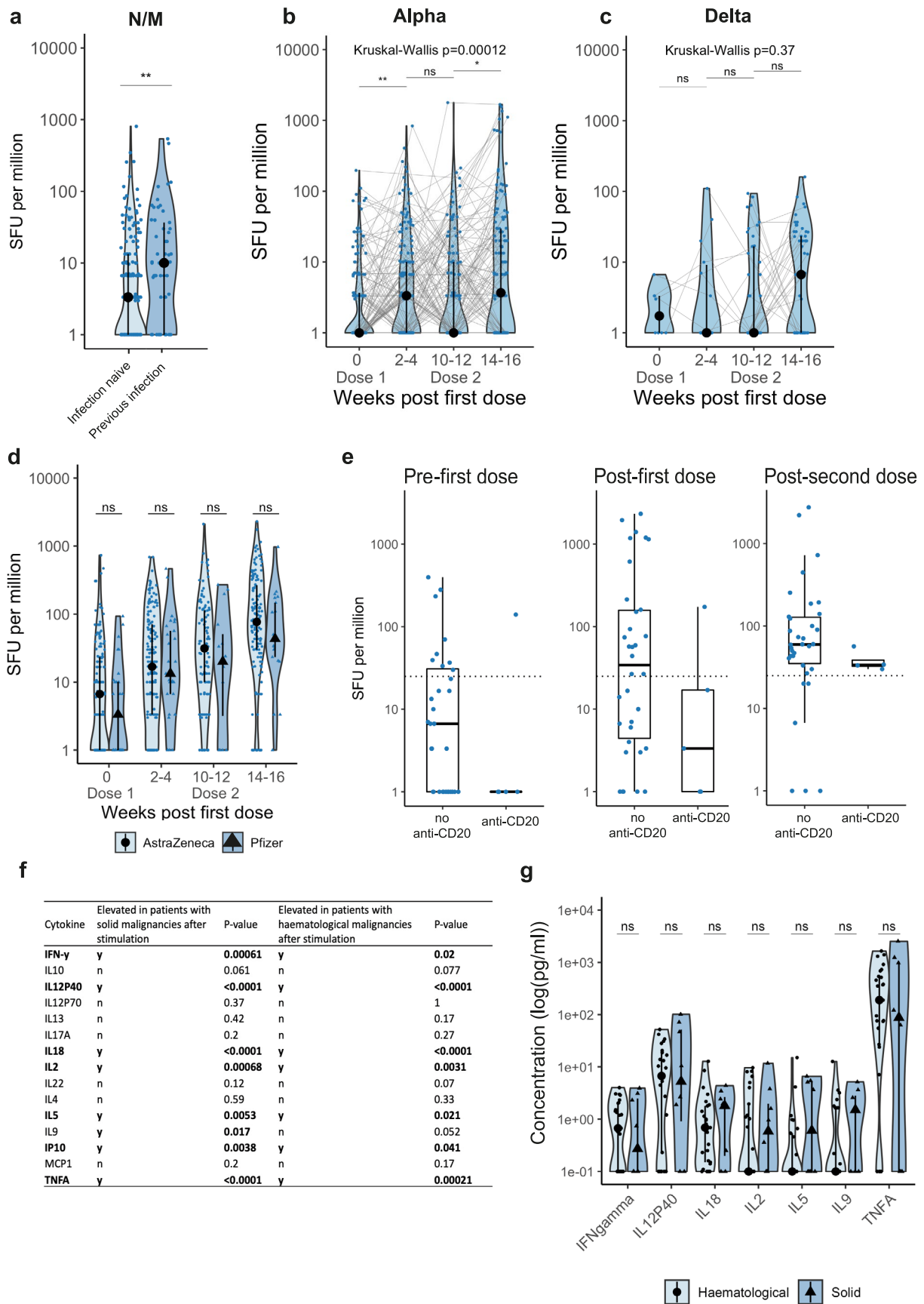


Extended Data Fig. 4 | Neutralising titres WT SARS-CoV-2 and VOCs in patients treated with anti-CD20. Comparison of neutralising titres against WT SARS-CoV-2, Alpha, Beta, and Delta in haematological patients treated with anti-CD20. Boxes indicate the 25 and 75 percentiles, line indicates the median, and whiskers indicate 1.5 times the IQR percentiles. Dots represent individual patient samples. Dotted lines indicate the lower and upper limit of detection. Significance was tested by two-sided Wilcoxon-Mann-Whitney U test, $p < 0.05$ was considered significant.



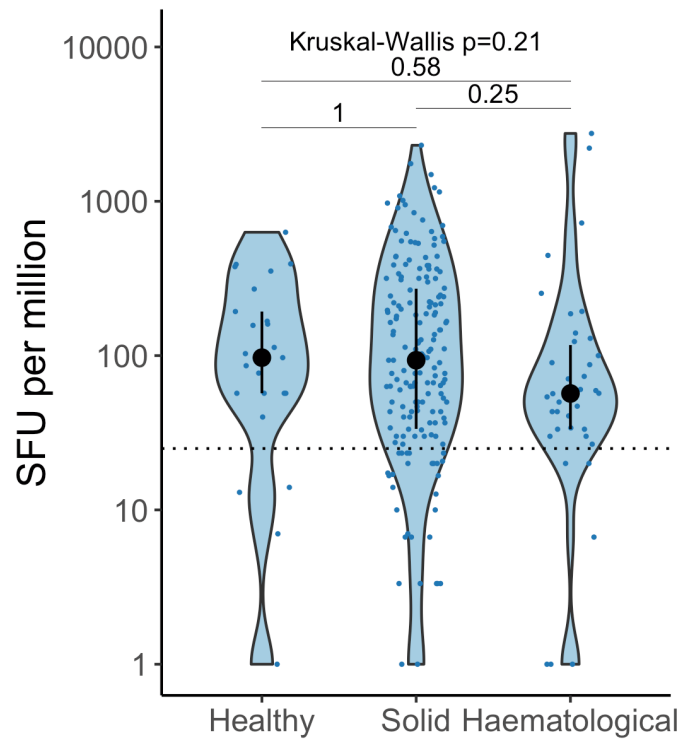
Extended Data Fig. 5 | See next page for caption.

Extended Data Fig. 5 | Neutralising responses in patients with cancer and healthy controls. a) NAbT against WT SARS-CoV-2, Alpha, Beta, and Delta in infection naive, healthy individuals (n = 55, by age: 39/16), patients with solid cancers (n = 48, by age: 9/39) and haematological malignancies (n = 24, by age: 5/19) after two doses of Pfizer. Median fold-decrease in NAbT is shown for each VOC in comparison to WT SARS-CoV-2. Dotted line at <40 denotes the lower limit of detection, dotted line at >2560 denoted the upper limit of detection. Violin plots denote density of data points. PointRange denotes the median and the 25 and 75 percentiles. Dots represent individual samples. Significance was tested by Kruskal Wallis test, $p < 0.05$ was considered significant, post-hoc test: two-sided Wilcoxon Mann-Whitney U test with Bonferroni correction was used for pairwise comparisons. ns, non-significant, * $p < 0.05$, ** $p < 0.01$, *** $p < 0.001$. **b)** NAbT were categorised as undetectable/low (<40), medium (40-256), or high (>256) are shown for WT SARS-CoV-2 and the three VOCs. Differences were analysed using Chi-Square test. p-values < 0.05 were considered significant. Patient numbers per category are annotated in graph. **c)** NAbT against WT SARS-CoV-2, Alpha, Beta, and Delta in, healthy individuals (n = 8), patients with solid cancers (n = 77) and haematological malignancies (n = 18) after two doses of AZ. Median fold-decrease in NAbT is shown for each VOC in comparison to WT SARS-CoV-2. Dotted line at <40 denotes the lower limit of detection, dotted line at >2560 denoted the upper limit of detection. Violin plots denote density of data points. PointRange denotes the median and the 25 and 75 percentiles. Dots represent individual samples. Significance was tested by Kruskal Wallis test, $p < 0.05$ was considered significant, post-hoc test: two-sided Wilcoxon Mann-Whitney U test with Bonferroni correction was used for pairwise comparisons. ns, non-significant, * $p < 0.05$, ** $p < 0.01$, *** $p < 0.001$. **d)** NAbT were categorised as undetectable/low (<40), medium (40-256), or high (>256) are shown for WT SARS-CoV-2 and the three VOCs. Differences were analysed using Chi-Square test. p-values < 0.05 were considered significant. Patient numbers per category are annotated in graph. NAbT, neutralizing antibody titre.

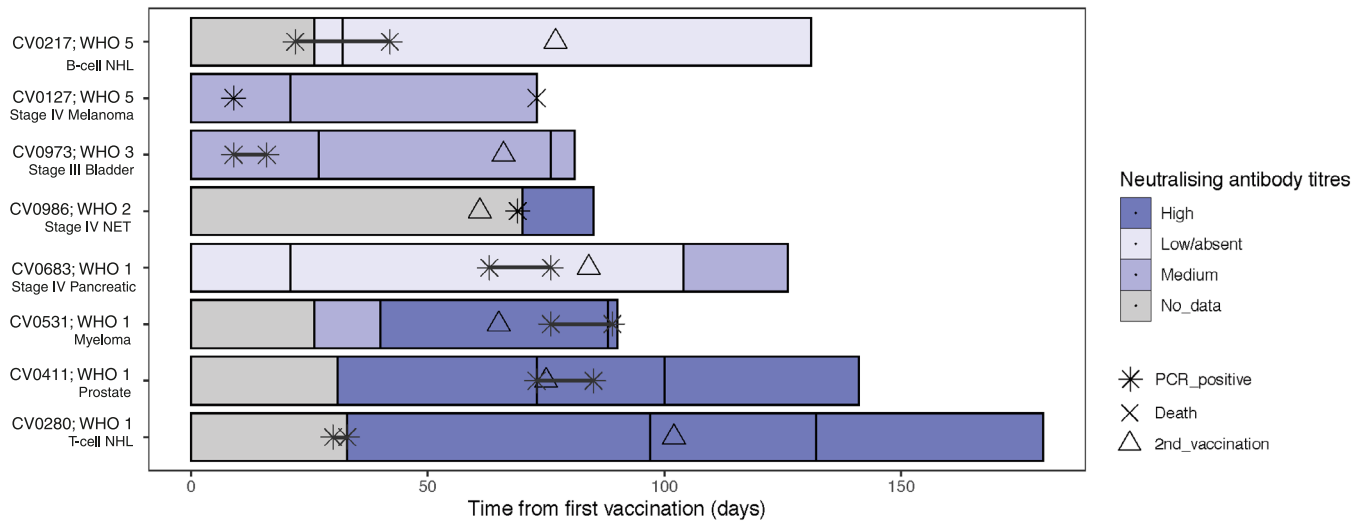


Extended Data Fig. 6 | See next page for caption.

Extended Data Fig. 6 | SARS-CoV-2-specific T-cell responses following COVID-19 vaccination. a) Comparison of SFU/10⁶ PBMC after stimulation with N and M peptide pools before vaccination in infection naïve (n=171) vs previously infected (n=56) patients. Significance was tested by two-sided Wilcoxon Mann-Whitney U test, p < 0.05 was considered significant. ** p < 0.01. SFU/10⁶ PBMC in infection naïve patients after stimulation with spike peptide pools specific to **b)** Alpha VOC (n=209/254/152/199 at BL/FU1/FU2/FU3), and **c)** Delta VOC (n=15/20/54/86 at BL/FU1/FU2/FU3). Violin plots denote density of data points. PointRange denotes the median and the 25 and 75 percentiles. Dots represent individual samples. Samples from individual patients are connected. Significance was tested by Kruskal Wallis test, p < 0.05 was considered significant, post-hoc test: two-sided Wilcoxon Mann-Whitney U test with Bonferroni correction was used for pairwise comparisons. Only comparisons with an adjusted p-value < 0.05 are denoted in the graph. * p < 0.05, ** p < 0.01, *** p < 0.001. **d)** Comparison of SFU/10⁶ PBMC in patients receiving AZ (n=194/216/146/187 at BL/FU1/FU2/FU3) vs PZ (n=41/46/27/42 at BL/FU1/FU2/FU3) vaccines. Violin plots denote density of data points. PointRange denotes the median and the 25 and 75 percentiles. Dots represent individual samples. Significance was tested by two-sided Wilcoxon-Mann-Whitney U test, p < 0.05 was considered significant. **e)** Comparison of SFU/10⁶ PBMC in haematological patients treated with anti-CD20 (Anti-CD20: n=5/5/4 at BL/FU1/FU3, No anti-CD20: n=32/35/37 at BL/FU1/FU3). Boxes indicate the 25th and 75th percentiles, line indicates the median, and whiskers indicate 1.5 times the IQR. Dots represent individual samples. Dotted lines indicate the limit of positivity. AZ, AstraZeneca; PBMC, peripheral blood mononuclear cells; PZ, Pfizer; SFU, spot-forming unit. **f)** Comparison of the levels of 15 cytokines in ELISPOT culture supernatants after stimulation with S1 and S2 peptide pools vs unstimulated controls. Significance was tested by two-sided Wilcoxon-Mann-Whitney U test, p < 0.05 was considered significant. **g)** Comparison of 7 cytokines in patients with haematological (n=25 patients) vs solid cancers (n=8 patients). Significance was tested by two-sided Wilcoxon-Mann-Whitney U test. BL, baseline; FU1, 21-56 days post first-vaccine; FU2, 14-28 days prior to second vaccine; FU3, 14-28days post second vaccine.



Extended Data Fig. 7 | SARS-CoV-2-specific T-cell responses in healthy controls. T-cell responses in healthy controls ($n=25$) and patients with solid ($n=188$) or haematological malignancy ($n=41$) after vaccination. T-cell responses are represented as the sum of SFU/ 10^6 PBMC after stimulation with WT S1 or S2 peptide pools. Dotted line at <24 denotes the threshold for positivity. Violin plots denote density of data points. PointRange denotes the median and the 25 and 75 percentiles. Dots represent individual samples. Samples from individual patients are connected. Significance was tested by Kruskal Wallis test, $p < 0.05$ was considered significant, post-hoc test: two-sided Wilcoxon Mann-Whitney U test with Bonferroni correction was used for pairwise comparisons. Only comparisons with the prior timepoint are denoted in the graph. ns, non-significant.



Extended Data Fig. 8 | Swimmer plot of 8 patients testing positive for SARS-CoV-2 following vaccination. Each lane represents a patient and is coloured to represent the results of NAbT to WT SARS-CoV-2 virus (Low/absent, <40 / <35 ; Medium, 40 - 256; High >256). Black vertical lines represent sampling timepoints. As we did not mandate collection of serial SARS-CoV-2 RT-PCR testing, viral shedding was estimated as the time from the first positive to the last positive SARS-CoV-2 RT-PCR test. COVID-19 severity is represented by the WHO Ordinal Scale (See Methods).